Opposite symmetry in the lithospheric structure of the Alboran and Algerian basins and their margins(Western Mediterranean): Geodynamic implications

Kumar Ajay[1], Fernàndez Manel[2], Vergés Jaume[3], Torné Montserrat[4], and Jimenez-Munt Ivone[2]

[1]ICTJA-CSIC
[2]CSIC
[3]Institute of Earth Sciences Jaume Almera
[4]Institute of Earth Sciences Jaume Almera, ICTJA-CSIC

November 16, 2022

Posted on 16 Nov 2022 — CC-BY-NC 4 — https://doi.org/10.1002/essoar.10504755.1 — This a preprint and has not been peer reviewed. Data may be preliminary.

Abstract

The geodynamic evolution of the Western Mediterranean for the past 35My is a matter of debate. Present-day structure and composition of the lithosphere and sublithospheric mantle may help in constraining the geodynamic evolution of the region. We use an integrated geophysical-petrological modeling to derive and compare the present-day thermal, density and compositional structure of the lithosphere and sublithospheric mantle along two NNW-SSE oriented geo-transects crossing the back-arc Alboran and Algerian basins, from onshore Iberia to the northern Africa margin. The crust is constrained by seismic experiments and geological cross-sections, whereas seismic tomography models and mantle xenoliths constrain the upper mantle structure and composition. Results show a thick crust (37km and 30km) and a relative deep LAB (130km and 150km) underneath the HP/LT metamorphic units of the Internal Betics and Greater Kabylies, respectively, which contrast with the 16km thick magmatic crust of the Alboran Basin and the 10km thick oceanic crust of the Algerian Basin. The sharp change in lithosphere thickness, from the orogenic wedge to the back-arc basins, contrasts with the gentler lithosphere thickening towards the respective opposed margins. Our results confirm the presence of detached slabs ˜400°C colder than upper mantle and a fertile composition than the continental lithospheric mantle beneath the External Betics and Saharan Atlas. Presence of detached quasi-vertical sublithospheric slabs dipping towards the SSE in the Betics and towards the NNW in the Kabylies and the opposed symmetric lithospheric structure support an opposite dipping subduction and retreat of two adjacent segments of the Jurassic Ligurian-Tethys realm.

Opposite symmetry in the lithospheric structure of the Alboran and Algerian basins and their margins (Western Mediterranean): Geodynamic implications

Ajay Kumar[1, 2], Manel Fernàndez[1], Jaume Vergés[1], Montserrat Torne[1], Ivone Jiménez-Munt[1]

[1]Group of Dynamics of the Lithosphere, Geosciences Barcelona,GEO3BCN-CSIC, Lluís Solé Sabarís s/n, 08028 Barcelona, Spain.

[2]Department of Earth and Ocean Dynamics, University of Barcelona, Barcelona, Spain.

Corresponding author: Ajay Kumar (akumar@geo3bcn.csic.es, ajay6763@gmail.com)

Keywords: Western Mediterranean, integrated geophysical-petrological modeling, lithospheric structure, Ligurian-Tethys slabs, dynamic topography

Highlights:

- Opposite symmetry of crust and lithosphere structure along the Alboran and Algerian basins and their margins with subduction related exhumed HP/LT metamorphic rocks.
- Subducted Ligurian-Tethys slabs beneath the Betics and Kabylies are ~400 ^{o}C colder and at least ~30 kg/m^3 denser than ambient upper mantle showing fertile chemical composition alike to oceanic lithosphere.
- The Eastern Betics and Greater Kabylies underwent mantle delamination during Mid-Late Miocene triggered by slab retreat of the subducted Ligurian-Tethys segments, and further slab tear/break-off.
- Slab tear/break-off caused the uplift of several hundred meters in the eastern Betics and Greater Kabylies and the closure of the Atlantic-Mediterranean corridor preceding the Messinian salinity crises.

Abstract

The geodynamic evolution of the Western Mediterranean for the past 35My is a matter of debate. Present-day structure and composition of the lithosphere and sublithospheric mantle may help in constraining the geodynamic evolution of the region. We use an integrated geophysical-petrological modeling to derive and compare the present-day thermal, density and compositional structure of the lithosphere and sublithospheric mantle along two NNW-SSE oriented geo-transects crossing the back-arc Alboran and Algerian basins, from onshore Iberia to the northern Africa margin. The crust is constrained by seismic experiments and geological cross-sections, whereas seismic tomography models and mantle xenoliths constrain the upper mantle structure and composition. Results show a thick crust (37km and 30km) and a relative deep LAB (130km and 150km) underneath the HP/LT metamorphic units of the Internal Betics and Greater Kabylies, respectively, which contrast with the 16km thick magmatic crust of the Alboran Basin and the 10km thick oceanic crust of the Algerian Basin. The sharp change in lithosphere thickness, from the orogenic wedge to the back-arc basins, contrasts with the gentler lithosphere thickening towards the respective opposed margins. Our results confirm the presence of detached slabs ~400ºC colder than upper mantle and a fertile composition than the continental lithospheric mantle beneath the External Betics and Saharan Atlas. Presence of detached quasi-vertical sublithospheric slabs dipping towards the SSE in the Betics and towards the NNW in the Kabylies and the opposed symmetric lithospheric structure support an opposite dipping subduction and retreat of two adjacent segments of the Jurassic Ligurian-Tethys realm.

Graphical abstract

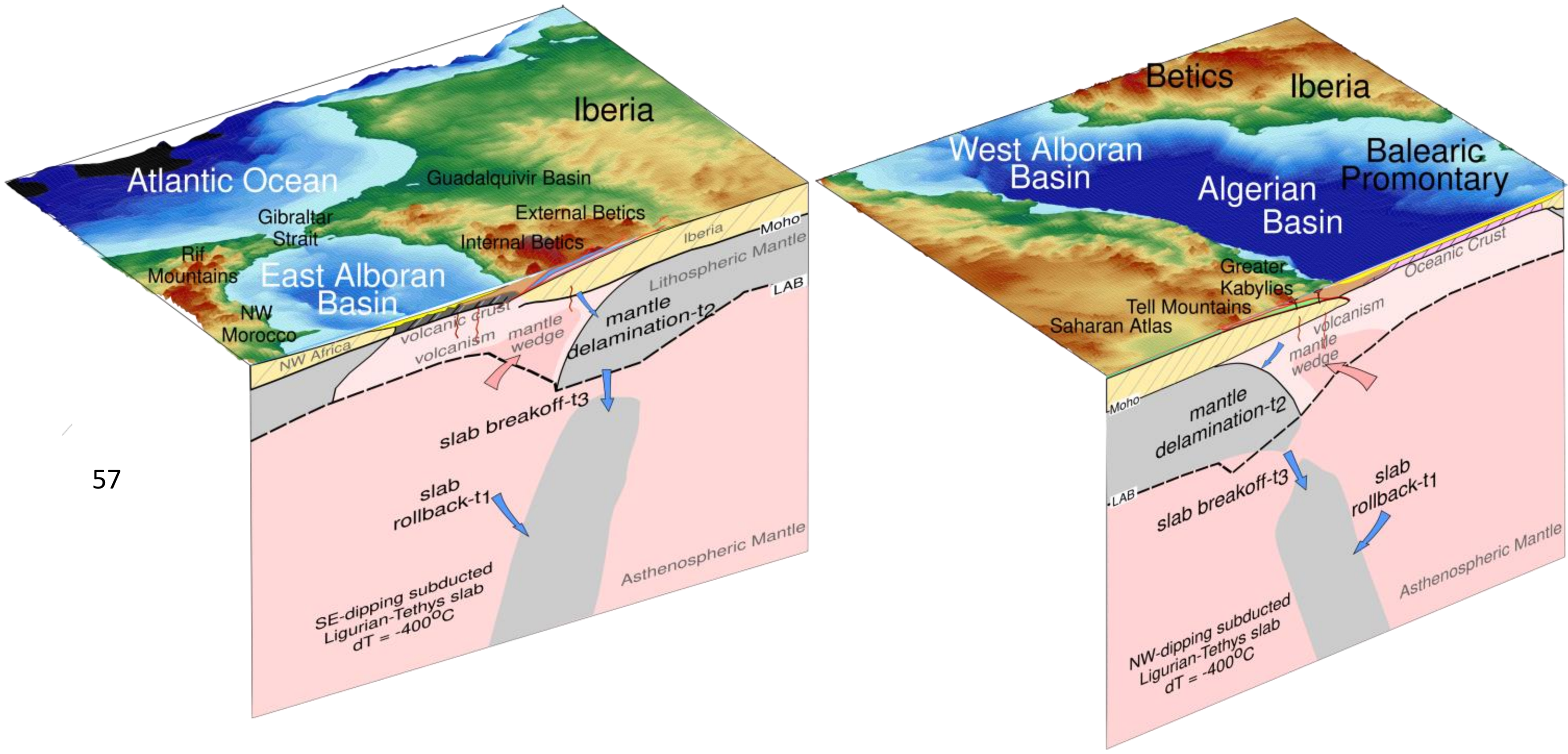
Atlantic Ocean
Iberia
Guadalquivir Basin
External Betics
Internal Betics
Gibraltar Strait
Rif Mountains
East Alboran Basin
NW Morocco
NW Africa
Iberia
Moho
Lithospheric Mantle
LAB
volcanic crust
volcanism
mantle wedge
mantle delamination-t2
slab breakoff-t3
slab rollback-t1
SE-dipping subducted Ligurian-Tethys slab dT = -400^{o}C
Asthenospheric Mantle
Betics
Iberia
West Alboran Basin
Balearic Promontary
Algerian Basin
Greater Kabylies
Tell Mountains
Saharan Atlas
Oceanic Crust
volcanism
mantle wedge
Moho
mantle delamination-t2
LAB
slab breakoff-t3
slab rollback-t1
NW-dipping subducted Ligurian-Tethys slab dT = -400^{o}C
Asthenospheric Mantle

1. Introduction

The Western Mediterranean is characterized by the presence of several extensional basins floored by very thin continental crust or newly formed oceanic crust that opened in a back-arc setting during the closure of the Ligurian-Tethys Ocean (Figure 1a). The North Balearic Transform Zone is recognized as a major transform fault separating the Liguro-Provençal Basin and the Tyrrhenian realm from the Alboran-Algerian realm (Figure 1a). While the Cenozoic evolution of the Liguro-Provençal, Tyrrhenian, and Aegean back-arc basins are well understood (Faccenna et al., 2004), the evolution of the Alboran and Algerian basins in the Western Mediterranean is still debated (Spakman and Wortel, 2004; Faccenna et al., 2004; Jolivet et al., 2009; Vergés and Fernàndez 2012; van Hinsbergen et al., 2014; Casciello et al., 2015). The opening of both basins for the last 35 My, is being explained by three different geodynamic scenarios, each based on slab roll-back as the driving mechanism (Figure 1b). There is consensus that the Algerian Basin is an oceanic basin opened in the upper plate during the NNW-dipping Ligurian-Tethys slab retreat, in agreement with the SSE-polarity of the Kabylies-Tell-Atlas orogenic system; however no agreement has been reached so far on the origin and evolution of the Alboran Basin and related Betic-Rif orogenic system. Main disagreements are on the original disposition of the tectono-sedimentary domains involved in the Betic-Rif subduction-related orogenic system and on the geodynamic interpretation used to build-up this orogenic system. The pros and cons of the three scenarios displayed in Figure1b are discussed in detail by Chertova et al. (2014) using numerical modeling and concluding that both scenario 1 and scenario 3 are plausible despite the authors favor scenario 1.

Irrespective of the geodynamic evolution model applicable to the Alboran and Algerian basins, subduction processes must have left their imprints on the present-day crust and mantle structure. A subduction system involves compression and orogenic volcanism near the arc. In settings dominated by slab roll-back, the upper plate undergoes extension and thinning, producing anorogenic volcanism by mantle decompression which ultimately can lead to the formation of new oceanic lithosphere as in the Algerian Basin. During the final stages of slab roll-back, collision with the continental lithosphere leads to the stacking and exhumation of metamorphic slices of the subducted thinned continental crust of the former extended margins (Brun and Faccenna, 2008). Involvement of the passive margin also introduces mechanical weakness and the dense slabs can break-off/tear/detach (Fernández-García et al., 2019). Hence, compression near the subduction front and extension in the back-arc are to be recorded in the present-day lithospheric thickness and mantle composition. Therefore, precise knowledge of the present-day lithospheric structure and chemical composition of the upper mantle are crucial constraints to decipher the geodynamic evolution of the study region.

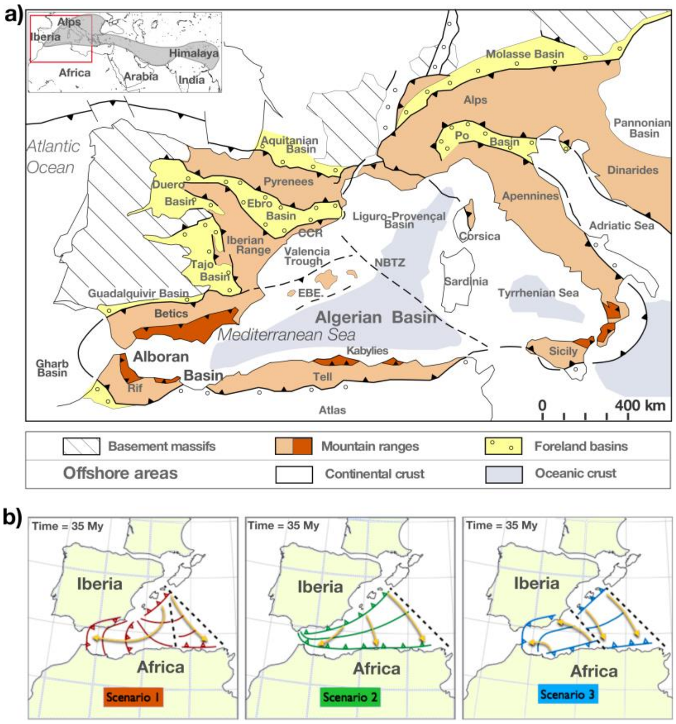

Figure 1. (a) Geological map of the Western Mediterranean showing the main orogenic belts and basins (Modified from Vergés and Sàbat, 1999).The Alpine-Himalayan collision zone is indicated as grey shaded area in the inset map. (b) Schematic illustration of the three subduction models proposed for the geodynamic evolution of the Western Mediterranean also showing the paleogeography at 35 My (van Hinsbergen et al. 2014). Scenario 1 after van Hinsbergen et al. (2014) purposes a single short subduction zone initially dipping to NW starting near the Balearic Promontory and then retreats to the SE before it separates into two different segment. One of the segments continue retreating to SE before it collides with North Africa and the other continue retreating to the west and collides with Iberia resulting in 180º clock-wise rotation. Scenario 2 purposes a long initial subduction dipping to the N-NW along the entire Gibraltar-Balearic Promontory margin (e.g., Gueguen et al., 1998; Faccenna et al., 2004; Jolivet et al., 2009). Scenario 3 after Vergés and Fernàndez (2012) purposes two separate subduction segments with opposite subduction and retreating direction for the Alboran (dipping to the SE and retreating to the NW) and Algerian (dipping to the NW and retreating to the SE) basins. Direction of rollback is shown by the yellow arrows. Black dashed lines represent the proposed transform faults separating the different subduction segments (Figure modified after Chertova et al., 2014). NBTZ, North Balearic Transform Zone; EBF, Emile-Baudot Escarpment.

The objective of this study is to derive and compare the present-day crust and upper-mantle structure (up to 400 km depth) of the Betics and Kabylies-Tell-Atlas orogenic systems, along two NNW-SSE oriented sections, hereinafter referred to as geo-transects, crossing the Alboran and Algerian back-arc basins and their opposed margins of North Africa and Iberia, respectively (Figure 2a). Orientation and location of the geo-transects are chosen based on: i) the regional vergence of the major tectonic units (Figure 2a), ii) available recent geophysical data (e.g., seismic tomography, active seismic lines and geological cross-sections), and iii) the different tectonic style, crustal nature, and lithospheric geometry of both basins. For this purpose, we model the present-day thermal, compositional, density and seismic velocity distribution along the Alboran and Algerian Basin geo-transects by combining surface heat flow (SHF), geoid height, Bouguer anomaly and elevation data in a self-consistent thermodynamic framework using the recently improved LitMod2D_2.0 code (Kumar et al., 2020).

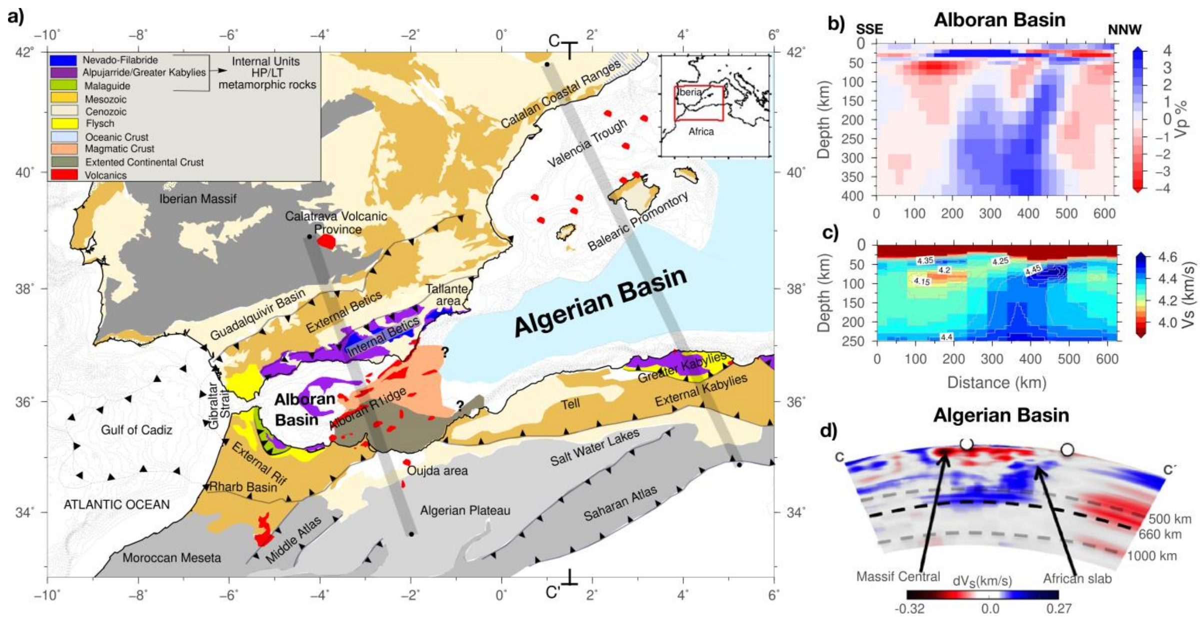

Figure 2. (a) Simplified geological map of the study region. Shaded grey lines show the location of the Alboran and Algerian basin geo-transects. (b) P-wave travel-time tomography along Alboran basin geo-transects from Bezada et al. (2013). (c) Absolute S-wave velocity model from Rayleigh surface wave dispersion (Palomeras et al. 2017) along the Alboran basin geo-transect. (d) S-wave tomography using full waveform inversion modified after Fichtner and Villaseñor (2015) along cross-section C-C' of Fichtner and Villaseñor (2015), see panel located in (a) for location.

The Alboran Basin geo-transect is presented for the first time while the Algerian Basin geo-transect follows the TRANSMED-II profile, that was modeled using a thermal approach (Roca et al., 2004), and later refined in Carballo et al. (2015a) using integrated geophysical-petrological modeling. Although the regional structure of the lithosphere across the region has already been studied by Fullea et al. (2010) and Carballo et al. (2015a and b), we focus here on a more detailed structure of the Betics and Greater Kabylies belts and offshore regions (i.e. Alboran and Algerian basins). LitMod2D_2.0 allows to model thermal/seismic/compositional sublithospheric mantle anomalies, thus allowing to incorporate the well imaged positive seismic velocity anomalies in the high resolution tomography beneath the Betics (Figure 2b; Bezada et al., 2013; Villaseñor et al., 2015; Palomeras et al., 2017) and the Kabylies (Figure 2d; Fichtner and Villaseñor, 2015). The models presented here also integrate the latest geophysical results mainly consisting of new active seismic data along the Algerian margin (e.g., SPIRAL, Aïdi, et al., 2018), and the Moroccan margin (Gómez de la Peña et al., 2018).

Finally, results are discussed in terms of the geodynamic implications for the closure of the Jurassic Ligurian-Tethys Ocean and the opening of the new oceanic and thinned continental domains of the Algeria and Alboran back-arc basins in an overall convergence regime that lasted for the past 85 My involving the African and European plates.

2. Geological summary

The Alboran and Algerian basins are located in the western end of the Alpine-Himalayan collision belt and constitute the Western Mediterranean in between Iberia and Africa (Figure 1a). The origin of both basins, like other Mediterranean basins, is linked to the roll-back of the subducted Ligurian-Tethys lithosphere (Gueguen et al., 1998; Jolivet and Faccenna, 2000; Faccenna et al., 2004; Royden and Faccenna, 2018). The Ligurian-Tethys rifting and subsequent ocean spreading started during Early-Middle Jurassic by the propagation of the Central Atlantic ridge separating Africa, Iberia and Adria. The Ligurian-Tethys transtensive rifting resulted in a highly extended and segmented Iberian and Africa margins transitioning to oceanic lithosphere to the east (Stampfli and Borel, 2002; Frizon de Lamotte et al., 2011;

Schettino and Turco, 2011; Vergés and Fernàndez, 2012; Fernàndez et al., 2019). The protracted N-NNW displacement of Africa relative to Eurasia since late Santonian was accommodated by the consumption of the Ligurian-Tethys oceanic domain. Roll-back processes linked to the subduction of the Ligurian-Tethys lithosphere under a slow rate of convergence between Africa and Iberia, led to the opening of the Alboran and Algerian back-arc basins and the development of the Internal-External Betics and Greater and Lesser Kabylies. The Iberia-Africa convergence was also responsible for significant intra-plate deformation leading to the uplift of the Iberian Chain, the Central System, the Catalan Coastal Ranges and part of the External Betics in Iberia; and the Tell and Atlas orogenic systems in North Africa (Vergés and Fernàndez 2006; Macchiavelli et al., 2017; Vergés et al., 2019)(Figure 2a).

Exhumation of high-pressure and low-temperature (HP/LT) metamorphic rocks is a typical process of roll-back subduction systems (e.g., Agard et al., 2018). Such metamorphic rocks, referred to as Internal Units in the literature, are found in the Betic-Rif orogen along the southern margin of Iberia and North Morocco, and in the Kabylies along the northern margin of Algeria (Figure 2a). The Betic-Rif orogenic system is a tightly curved mountain chain with a WSW-ENE orientation along the southern Iberian margin changing to N-S and NNW-SSE orientation in North Morocco. The orogen consists of a typical subduction-related fold and thrust belt, which from the External to Internal Units is formed by the Guadalquivir and Rharb flexural foreland basins, the External Units, the Flysch Units, the Internal Units, and the extensional back-arc Alboran Basin (see the structural style of these units in e.g., Balanyá and García-Dueñas, 1987; Michard et al., 2002; Frizon de Lamotte et al., 2004; Booth-Rea et al., 2005; Vergés and Fernàndez, 2012; Platt et al., 2013). The HP/LT metamorphic rocks of the Betics Internal Units from bottom to top are the Nevado-Filabride, the Alpujarride and the Malaguide (Figure 2a). The Rif Internal Units shows a similar tectonic architecture except for the lack of the equivalent Nevado-Filabride unit. The northern margin of Algeria shows similar characteristics but opposite spatial association compared to the Betic-Rif orogen (Figure 2a). The main tectonic units, from internal to external, are the extensional back-arc Algerian Basin, the HP/LT Internal Units rocks in the Kabylies followed by the thrusting of the

Flysch Units over the External Units, and farther to the SE, the fold and thrust belt in the Tell-Atlas Mountains (see the structural style in Khomsi et al., 2019).

The basement in the Alboran Basin changes from West to East (Figure 2a). The Western Alboran basin is floored by thin continental crust, including the HP/LT Alpujarride metamorphic basement units (Soto and Platt, 1999), and numerous volcanic intrusions (Gómez de la Peña et al., 2018); whereas the Eastern Alboran basin is mostly floored by magmatic crust (Booth-Reaet al., 2007). South of the Alboran Ridge, situated in the middle of the Alboran Basin, the basin is floored by an African continental crust with magmatic intrusions (Gómez de la Peña et al., 2018). The magmatic crustal domain of the Eastern Alboran Basin transitions eastward to the oceanic crust of the Algerian Basin (Pascal et al., 1993; Booth-Rea et al., 2007). The Valencia Trough, situated NNW of the Algerian Basin, in between the Catalan Coastal Ranges and the Balearic Promontory, has a very thin continental basement (Pascal et al., 1992; Torné et al., 1992), which experienced a huge extension during Mesozoic (Roca, 2001; Etheve et al., 2018). The trough underwent compression in late Palaeogene during the convergence between Africa and Iberia, and renewed extension from Late Oligocene to Langhian period (Fernàndez et al., 1995; Roca, 1996; Torné et al., 1996; Sàbat et al., 1997; Gaspar-Escribano et al., 2004). The basement of the Balearic Promontory is continental, similar to the Iberian basement beneath the Catalan Coastal Ranges (Pascal et al., 1992; Torné et al., 1992; Vidal et al., 1998).

Volcanism in the Western Mediterranean has been a focus of numerous studies (Martí et al., 1992; Duggen et al., 2005, 2008; Lustrino and Wilson, 2007; Lustrino et al., 2011; Melchiorre et al., 2017). In the Alboran Basin, volcanism is mainly orogenic with wide geochemical variation (Lustrino et al., 2011) showing tholeiitic Miocene affinity in its central region surrounded by calc-alkaline volcanism (Duggen et al., 2008). The southern Iberian (e.g., Tallante area) and north-western African (e.g., Oujda area) continental margins show Lower Pliocene to Upper Miocene Si-K-rich (i.e., orogenic) and Upper Miocene to Pleistocene Si-poor (i.e., anorogenic or intra-plate volcanism) magmatism (Duggen et al., 2005). The northern coast of Algeria, along the Algerian Basin, experienced K-rich (and minor medium-K) calc-alkaline volcanic activity (i.e., orogenic) along a ~450 km long E-W trending zone during Miocene (17 to 11 Ma) (Maury et al., 2000; Fourcade et al., 2001; Laouar et al., 2005). The younger anorogenic volcanism (alkaline) is observed in the eastern and western end of the Tell Mountains (Wilson and Bianchini, 1999; Maury et al., 2000; Coulon et al., 2002). The Valencia Trough experienced calc-alkaline volcanism (i.e., orogenic) in the Early-Middle Miocene and alkaline volcanic activity (i.e., anorogenic) from Middle Miocene to Recent (Martí et al., 1992).

3. Methodology and modeling parameters

We use the improved LitMod2D_2.0 code (Kumar et al., 2020), which integrates geophysical and petrological data to model the thermo-chemical structure of the crust and the upper mantle down to 400 km. The code, based on Afonso et al. (2008), solves the present-day 2D temperature, density (i.e., chemical composition) and seismic velocity structure by solving stable mantle phase and mineral assemblages using a Gibbs free-energy minimization algorithm and fitting simultaneously SHF, geoid height, Bouguer anomalies, and absolute elevation. Each of these surface observables is sensitive to the thermo-physical properties of the materials under study, which in turn depend on temperature, pressure, and composition. Moreover, since they have a distinctive sensitivity to shallow/deep and thermal/compositional density anomalies, the approach allows for better control of thermal and compositional density variations at different depths.

The model consists of different crustal and mantle bodies, characterized by individual thermo-physical properties and chemical composition, respectively. Crustal thermo-physical properties are taken from literature (Table 1), while its structure is constrained from geological cross-sections, and active and passive seismological experiments (i.e., crustal layers and Moho depth), that later are refined within the uncertainty limits to fit the regional surface observables. The depth of the lithosphere-asthenosphere boundary (i.e., LAB depth) is constrained by seismic tomography and the chemical composition of the lithospheric mantle (i.e. lateral compositional domains) is obtained from mantle xenolith data, crustal age-based lithospheric composition (Griffin et al., 2009), and geodynamic criteria. For mantle bodies, major oxides composition (Table 2) is assigned in the Na_2O-CaO-FeO-MgO-Al_2O_3-SiO_2 (NCFMAS) thermodynamic system. Stable phases and mineral assemblages are computed using the Gibbs free-energy minimization algorithm (Connolly, 2005, 2009) within upper mantle pressure and temperature ranges. To that purpose, we use an augmented-modified version of Holland and Powell (1998) thermodynamic database (Afonso and Zlotnik, 2011) in which pressure, temperature, and composition-dependent bulk rock density, elastic parameters, and thermal conductivities are calculated using a rule of mixture. Seismic velocities corrected for anelastic attenuation are calculated from the bulk and shear modulus using the parameters from Jackson et al. (2010) and the formulation from Afonso et al. (2008). Temperature distribution is calculated under the assumption of steady-state by solving the heat transport equation using finite-elements, with prescribed boundary conditions at the surface (0 ºC) and at the LAB (1320 ºC). In the lithospheric mantle, temperature, pressure, and composition-dependent thermal conductivities are used. The temperature gradient below the thermal buffer layer is restricted to $0.35 \leq dT/dz \leq 0.50$ °C/km. In order to incorporate relative velocity anomalies in the sublithospheric mantle (i.e., subducted slabs) the prescribed amount of the seismic velocity anomaly is converted to thermal anomaly (ΔT) which then is added to the adiabatic thermal gradient and the thermo-physical properties from the assigned chemical composition are recalculated at new ($T+\Delta T$, P) conditions.

Table 1. Thermo-physical properties of the different tectonic units in the crust along the geo-transects. Densities are assigned according to previous studies (e.g., Carballo et al., 2015a and b) and using velocity-density envelops defined in Brocher (2005). The densities of the HP/LT units result from modeling (see Figure S1). Thermal conductivities are taken from previous studies (e.g., Torne et al., 2000, 2015; Teixell et al., 2005; Zeyen et al., 2005; Carballo et al., 2015a and b), and radiogenic heat production comes from direct measurements in the Iberian Massif and Betics (Fernàndez et al., 1998a) and a global compilation of relevant crustal rocks (Vilà et al., 2010).

Tectonic units		**Density** (kg/m^3)	**Thermal Conductivity** (W/K·m)	**Radiogenic Heat Production** (µ.W/m^3)
Sediments	Neogene sediments	2400	2.2	1.0
	Neogene/Mesozoic sediments	2600	2.4	1.0
	Mesozoic sediments	2650	2.5	1.0
Betics	Nevado-Filabride	2900	2.5	1.0
	Alpujarride	2850*	2.5	1.0
	External Units	2600*	2.5	1.2
Greater Kabylies	Internal Units	2900*	2.5	1.0
	External Units	2600*	2.5	1.2
Continental crust	Upper crust	2750	2.4	1.65
	Middle crust	2850	2.1	0.5
	Lower crust	2950	2.0	0.2
Volcanic crust		2820	2.1	0.2
Oceanic crust		2950	2.5	0.3

*Calculated as a function of pressure using $\rho = \rho_o (1+ \beta P)$ where ρ_o is the density at the surface, β is the isothermal compressibility ($10x10^{-11}Pa^{-1}$ for the External units and $3x10^{-11}Pa^{-1}$ for the Internal Units), and P is the pressure in Pa.

Table 2. Major oxides composition (weight %) in the NCFMAS system for the lithospheric mantle and sublithospheric domains used in the modeling and corresponding relevant physical properties at given pressure and temperature.

Name	SiO_2	Al_2O_3	FeO	MgO	CaO	Na_2O	#Mg(100 xMgO/[MgO+FeO])	ρ(kg/m^3)		V_P&V_S (km/s)	
								at P=3GPa (~ 100km) T=1300 ^oC	at P= 6GPa (~ 200km) T=1400^oC	at P=3GPa (~ 100km) T=1300 ^oC	at P= 6GPa (~ 200km) T=1400^oC
PUM	45.0	4.5	8.1	37.8	3.6	0.36	89.3	3310	3396	7.986 4.441	8.254 4.523
DMM	44.70	3.98	8.18	38.73	3.17	0.13	89.4	3307	3391	7.950 4.396	8.232 4.491
DMM - 3%	44.59	3.51	8.21	39.63	3.02	0.082	89.58	3300	3385	7.936 4.390	8.222 4.488
DMM - 6%	44.47	3.08	8.23	40.53	2.78	0.051	89.72	3294	3378	7.929 4.388	8.211 4.484
DMM - 7%	44.43	2.97	8.23	40.78	2.70	0.045	89.77	3293	3376	7.927 4.388	8.209 4.484
Tc_1	44.5	3.5	8.0	39.79	3.1	0.24	89.86	3296	3381	7.934 4.391	8.213 4.488
Pr_6	45.4	3.7	8.3	39.9	3.2	0.26	90.6	3299	3385	7.931 4.388	8.213 4.486
CVP	44.51	3.76	8.75	37.89	3.28	0.36	91	3309	3395	7.909 4.374	8.194 4.473

PUM, Primitive Upper mantle (McDonough and Sun, 1995); DMM, Depleted mid-oceanic-ridge-basalt Mantle (Workman and Hart, 2005); Tc_1, Average Garnet Tecton (Griffin et al., 2009); Pr_6,Average Proton Lherzolite (Griffin et al., 2009; Le Roux et al., 2007); CVP, Calatrava Volcanic Province (Villaseca et al., 2010)

The final density distribution in the model is obtained with an iterative scheme to include the effect of pressure, temperature and composition. From the final density distribution, gravity anomalies (Bouguer), and geoid height are calculated. Seismic velocities in the mantle are assigned according to stable mineral assemblages at corresponding pressure and temperature and are compared with available seismic velocity and tomography models. Elevation under the assumption of isostatic equilibrium is calculated referenced to an old oceanic lithosphere column with a compensation level at 400 km depth (for details see Kumar et al., 2020). Flexural contribution to the short-wavelength elevation is calculated by considering an elastic thickness and load distribution resulting from the pressure variations at the compensation level along the geo-transect, following the procedure described in Jiménez-Munt et al. (2010) and using the code tAo (García-Castellanos et al., 2002). Mantle flow associated with sublithospheric mantle anomalies (i.e., subducted slabs) can produce dynamic topography affecting the absolute elevation. These dynamic effects are incorporated by calculating two end members of elevation: 1) full mechanical coupling of sublithospheric bodies to the overlying lithosphere (coupled elevation), and 2) no mechanical coupling of sublithospheric bodies to the lithosphere (uncoupled elevation). Consequently, uncoupled anomalies do not influence the calculated isostatic elevation but do affect geoid height, gravity anomalies and mantle seismic velocities.

The integrated geophysical-petrological modeling utilized in this study assumes thermal steady-state regime without advection. Although this assumption is valid for old tectono-thermal regions (>100 Ma) it is less valid in the Western Mediterranean where tectonic deformation is more recent (Cenozoic). Despite this, the results are constrained by the simultaneous fitting of a set of “instantaneous” density-dependent observables such as gravity, geoid and elevation. Hence, the results must be considered as a snapshot of the present-day density distribution related to active tectonic processes. In regions affected by thermal relaxation after lithospheric thinning, the actual temperature at Moho depth levels is higher than that calculated assuming thermal steady-state because the mass deficit associated with the transient thermal perturbation must be compensated by a larger lithospheric thickness to keep elevation. Therefore, steady-state modeling tends to underestimate the Moho temperature and overestimate the actual lithospheric thickness in regions of lithospheric thinning showing the opposite effects where the lithosphere is thickened (Fullea et al., 2007). Temperature and density distribution could be improved using a transient thermal model but this requires a more sophisticated numerical approach (i.e., solving the diffusion and advection terms in the heat flow equation) and, more importantly, an in-depth knowledge of the past and ongoing geodynamic processes and particularly, their evolution through time.

4. Data

4.1 Regional geophysical data

Alboran Basin geo-transect

Onshore Iberia, elevation increases from 500 m in the Iberia Massif to as much as ~2500 m in the eastern Internal Betics, coinciding with a decrease of the Bouguer anomaly to values of -120 mGal (Figure 3). Geoid height also decreases from 6–7 m in the southwestern Iberian Massif to 3–0 m in the western Betics and the Guadalquivir Basin, respectively. A local geoid high of 6 m is observed in the eastern Internal Betics where elevation attains its maximum values (Figures 3a and c). The Alboran Basin shows positive Bouguer anomalies, except in its westernmost end where large accumulations (up to 8–9 km) of Oligocene to Recent sediments are recorded. An ENE-WSW relative high delineates the central region of the basin, increasing up to 160 mGal in its easternmost end, in the transition to the oceanic crust of the Algerian Basin. Along the geo-transect, Bouguer anomalies decrease asymmetrically from the axis of the basin to the onshore regions. While to the Iberian margin gravity anomalies decrease rapidly. We observe a gentler decrease towards the African margin and the Algerian Plateau where values of -90 mGal are achieved (Figure 3b). The geoid height in the Alboran Basin shows a saddle point of ~3 m in its central region decreasing asymmetrically to the east and west and increasing in an N-S direction, with values of 5–6 m onshore Iberia and > 7 m in the Algerian Plateau (Figure 3c). This saddle region of the geoid height delineates the magmatic arc region and the North African continental margin block, and separates the prominent geoid low associated with the Gulf of Cadiz accretionary wedge and the West Alboran fore-arc basin to the Algerian back-arc oceanic basin. Interestingly, geoid height and elevation along the geo-transect follow a similar regional trend characterized by a rapid increase from the centre of the basin to the Internal Betics with local highs of 6 m and >2000 m, respectively, and a smoother increase towards the Algerian Plateau, where geoid and elevation attain values of up to 8 m and 1000 m, respectively. On the contrary, the Bouguer anomaly does not record a similar local high; instead we observe a rapid decrease from the gravity high of central Alboran Basin to the gravity low of the Internal Betics. Surface heat flow data (Figure 3a), though sparse, shows relatively higher values in the Alboran Basin increasing from west to east towards the Algerian Basin. Onshore Iberia shows lower SHF (~48 mW/m^2) than the onshore north Africa (~100 mW/m^2).

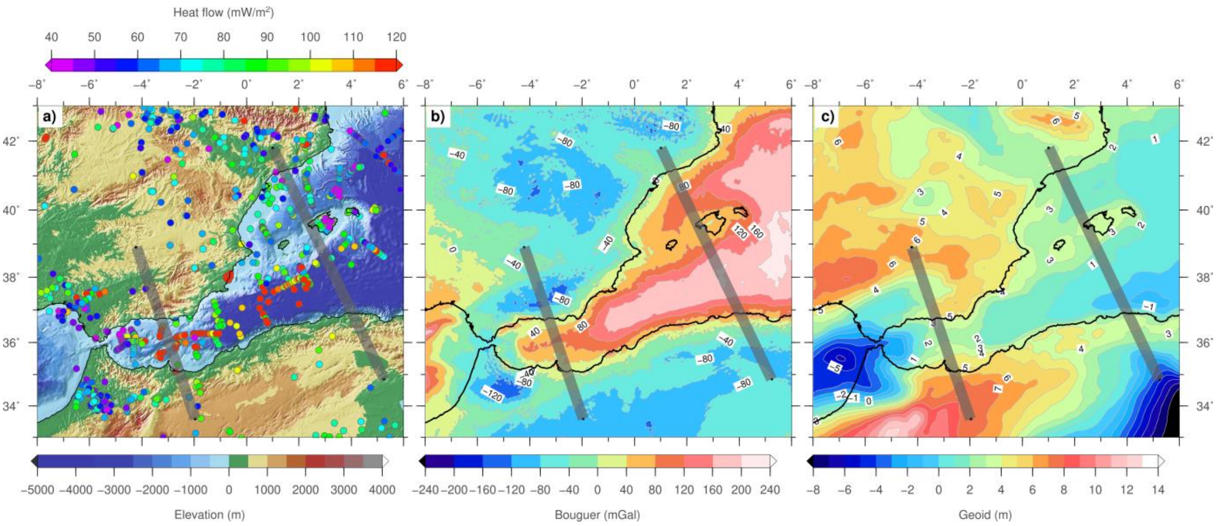

Figure 3. Geophysical observables in the region. (a) Shaded elevation and surface heat flow (dots). Elevation data from ETOPO1 (Amante and Eakins, 2009; http://www.ngdc.noaa.gov/mgg/global/global.html). Surface heat-flow (SHF) data have been compiled from Fernàndez et al. (1998b), Foucher et al. (1992), Marzán (2000), Poort et al. (2020), Rimi et al. (2005), and the International Heat Flow Commission global data set for Algeria (https://www.ihfc-iugg.org/products/global-heat-flow-database). (b) Bouguer anomaly map. Data for Iberia comes from Ayala et al. (2016). For Africa and offshore regions, Bouguer gravity anomalies are calculated by applying the complete Bouguer correction to free air satellite data (Sandwell and Smith, 1997, updated 2007) using FA2BOUG code (Fullea et al., 2008) with a reduction density of 2670 kg/m^3. (c) Geoid height from ICGEM (Ince et al., 2019; http://icgem.gfz-potsdam.de) where we used the GECO model (Gilardoni et al., 2016) filtered up to degree and order 10. Grey thick lines show the locations of the modeled NNW-SSE oriented geo-transects.

Algerian Basin geo-transect

In the interior regions of the Tell Mountains and Salt Waters Lakes, elevation ranges from 500 m to 1000 m, with a local low located at the SE end of the geo-transect, whereas Bouguer anomalies are in the range of 40–80 mGal decreasing towards the Saharan Atlas. Geoid shows values of ~3–4 m in the Tell Mountains that rapidly decrease to the SE where a prominent regional geoid low is located (Figure 3c). Along the geo-transect, local highs of elevation and Bouguer anomaly are observed in the Greater Kabylies and Tell-Atlas Mountains that coincide with a geoid regional high. The Bouguer anomaly increases abruptly from 60–80 mGal close to the Africa shoreline to above 160 mGal in the central regions of the Algerian Basin indicating the pronounced crustal thinning along the continental slope and slope break, and the oceanic nature of the crust in the central Algerian Basin. Elevation and geoid abruptly decrease to values of < -3000 m and 0–1 m in the slope break, values that characterize the central regions of the basin.

A very abrupt increase of elevation is observed along the Emile-Baudot Escarpment that marks the southeast termination of the Balearic Promontory, a ~350 km long and 105–155 km wide topographic feature with an average elevation of 500 m that separates the Valencia Trough, to the northwest, from the Algerian Basin, to the southeast. The Promontory is characterized by a smooth decrease of the Bouguer anomaly and an increase of geoid height (Figures 3b and c). Elevation and geoid decrease towards the central region of the Valencia Trough coinciding with an increase of the gravity anomalies indicating the presence of a thinned continental crust. SHF data exhibit a wide scatter around a mean value of 65 mW/m^2 onshore eastern Iberia increasing to 70–90 mW/m^2 in the Valencia Trough and decreasing again to the Balearic Promontory, where measurements are strongly affected by shallow groundwater circulation (Fernàndez and Cabal, 1992). Along the geo-transect, SHF data show a very poor coverage in the Algerian Basin and onshore Africa. Nevertheless, seafloor heat flow measurements carried out in the western Algeria Basin show values ranging from 90 mW/m^2 to 120 mW/m^2 (Marzán, 2000) (Figure 3a). In summary both basins show a rather similar regional pattern of the surface observables, the main difference being their amplitude that reflects the different stages of their evolution. While back-arc extension in the Algerian Basin progressed to the onset of new oceanic crust, in the Valencia Trough extension resulted in noticeable crustal thinning that progresses in a SW-NE direction towards the Ligurian-Provençal Basin.

4.2 Crustal data

The initial crustal geometry along the geo-transects is based on geological maps and cross-sections, and active and passive seismic data. Along the Alboran Basin geo-transect the crustal structure in the Iberian Massif is mainly based on the ALCUDIA2 Wide-Angle Seismic Reflection Transect (Ehsan et al., 2015). In the Guadalquivir Basin and Betics (Internal and External), seismic data come from different experiments (e.g., Banda et al., 1993; Comas et al., 1995; Gallart et al., 1995; Carbonell et al., 1997) and geological cross-sections (e.g., Banks and Warburton, 1991; Berástegui et al., 1998; Frizon de Lamotte et al., 2004; Michard et al., 2002; Platt et al., 2003b; Ruiz-Constan et al., 2012). Crustal data in the Alboran Basin and North Africa margin come from active seismic lines processed and interpreted in Gómez de la Peña et al. (2018). In addition to these data, the Moho depth along the geo-transect is also constrained by active and passive seismic data compilation (Diaz et al., 2016), joint inversion of elevation and gravity (Torne et al., 2015; Globig et al., 2016), surface wave dispersion tomography (Palomeras et al., 2017) and previous integrated geophysical-petrological modeling (Fullea et al., 2010; Carballo et al., 2015a and b) (Figure 4a).

The crustal geometry along the Algerian Basin geo-transect, except for the onshore northern Africa margin, is well known from the numerous deep seismic reflection and wide-angle/refraction profiles collected during the last decades (Figure 4b). Moho depths in the Valencia Trough and the Balearic Promontory are taken from Torne et al. (1992) and Pascal et al. (1992), while the crustal structure is summarized in the TRANSMED-II transect (Roca et al., 2004) and Carballo et al. (2015a). For the sake of completeness, original seismic data come from VALSIS-II (Torne et al., 1992), ESCI-Valencia (Vidal et al., 1998), Hinz (1972) and ALE-4 (an industry transect) in the Algerian Basin. In the North Africa margin, crustal structure is taken from the SPIRAL active seismic experiment (Aïdi et al., 2018) and further south from the geological cross-section of Frizon de Lamotte et al. (2011). Onshore, in the Catalan Coastal Ranges, receiver function and deep seismic sounding Moho depths are taken from Diaz et al. (2016).

4.3 Mantle structure and chemical composition

The depth to the base of the lithosphere (LAB), the chemical composition of the defined lithospheric domains, and the sublithospheric mantle anomalies are constrained by available tomography studies, geochemical analyses from mantle xenoliths and exhumed rocks, and previous modeling results. Initial LAB depths along the geo-transects come from previous 2D and 3D lithospheric models using elevation, gravity and geoid height, based on pure thermal and geophysical-petrological approaches (e.g., Fullea et al., 2010; Carballo et al., 2015a and b; Torne et al., 2015; Globig et al., 2016) and, in the case of the Alboran Basin geo-transect, also from the regional seismic tomography model by Palomeras et al. (2017).

In the onshore regions (Iberia and north Africa), lithospheric mantle compositional domains are taken from the previous studies in the same zone, which are based on mantle xenoliths, exhumed mantle rocks or tectono-thermal age of the crust (e.g., Griffin et al., 2009; Fullea et al., 2010; Carballo et al., 2015a and b; Jiménez-Munt et al., 2019). In the Algerian and Alboran basins, the Valencia Trough, and the Kabylies and Betics, mantle chemical composition is calculated from the major oxides partition as a function of aggregate melting using the empirical formulation of Niu (1997). One of the main novelties of this study is that we use a depleted mid-oceanic-ridge-basalt mantle composition (DMM; Workman and Hart, 2005) for the sublithospheric mantle, which as pointed out by Kumar et al. (2020), allows to reproduce the P-wave velocities of ak135 model (from 35 to 250 km depth) and resolves the mismatch between thermodynamically calculated seismic velocities and those from ak135 below 250 km depth.

5. Results

Here, we present the results of the lithospheric structure and thermo-physical properties of the upper mantle along the geo-transects derived from the 2D integrated geophysical-petrological modeling approach. Surface observables (SHF, geoid height, Bouguer anomaly and elevation; Figure 3) are projected onto the geo-transects at 5 km sampling interval within a strip of 25 km half-width to account for lateral variations perpendicular to the strike of the geo-transects. The standard variations are used as error bars associated with the observables (Figures 5 and 7). The crustal structure is well constrained in most segments of the geo-transects, and is slightly modified when strictly necessary to match the surface observables after changing the geometry and composition of the less constrained mantle domains.

Nevertheless, modifications of the crustal model are always within the uncertainties of the experimental data. The boundaries of the sub-crustal bodies must be considered as transition zones where the properties of the mantle (composition, seismic velocities and temperatures) change gradually rather than abruptly.

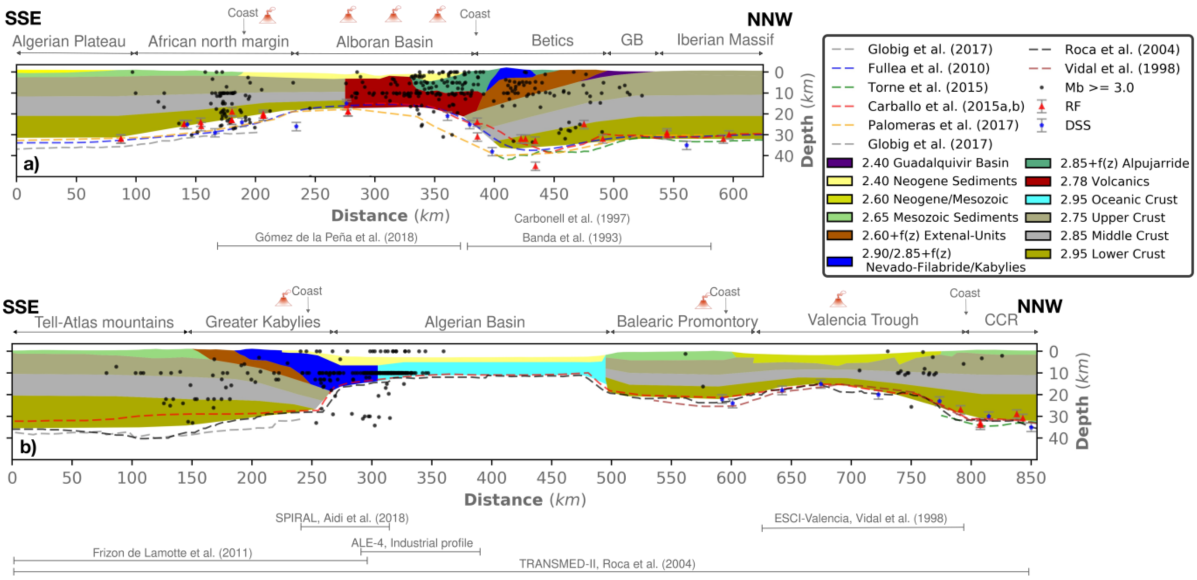

Figure 4. Crustal structure corresponding to the best fitting model for the (a) Alboran Basin and (b) Algerian Basin geo-transects. Densities used in each body are color-coded (see the legend). Moho depths from previous studies (including active seismic, receiver functions, surface wave dispersion and joint modeling of gravity and elevation) are plotted for comparison. Earthquakes (Mb ≥ 3.0; 1964-2016, ISC catalogue, https://doi.org/10.31905/D808B830) projected 50 km across the geo-transects are plotted with filled black circles. Note that the y-axis is exaggerated by two times the x-axis for better visualization. GB, Guadalquivir Basin; CCR, Catalan Coastal Ranges; RF, Receiver functions; DSS, Deep seismic sounding.

5.1. The Alboran Basin geo-transect: structure, temperature, and density

5.1.1 Crust and upper mantle structure

The crust of the Iberian and African mainland and their margins has been modeled using a three-layer crustal model; upper, middle and lower crust (Table 1 and Figure 4a). In the Iberian Massif the crust is ~32 km thick, which is consistent with previous studies, and thickens up to ~37 km below the Internal Betics over a distance of 100 km (Figure 4a). The Guadalquivir foreland basin reaches a maximum depth of 4 km close to the Betics fold and thrust belt front and dips southwards. The structure of the External Betics is constrained by low seismic velocity at crustal levels as observed in local seismic tomography models (Carbonell et al., 1998; Moudnib et al., 2015), while the structure of the Nevado-Filabride and the Alpujarride Internal Units are mainly defined from geological observations (Figure 4a). These two tectonically stacked HP/LT Betics Internal Units are defined as high density tectonic nappes according to P-T conditions of their metamorphic facies and densities of their basement and cover protoliths after metamorphic peaks (e.g., Gómez-Pugnaire et al., 2019) (Figure S1). The Nevado-Filabride, at the base of the thrust sheet pile, forms an open and elongated dome that is overlaid to the N by the Alpujarride thrusts. To the SE, the Alpujarride Unit is slightly dipping towards the Alboran Basin and thus forming the basement of the Neogene sedimentary infill in the proximal Iberian margin. The crust of the Alboran Basin is modeled as a highly intruded volcanic domain cropping out near the Alboran Ridge (Gómez de la Peña et al., 2018). The thinnest crust along the entire geo-transect is found in the Alboran Basin with Moho depths of 16–17 km being consistent with previous estimates (Figure 4a). Southeast of the Alboran Ridge, the crust is interpreted as African continental crust of about 18 km thickness, with thinning localized mainly at mid- and lower-crustal levels (Gómez de la Peña et al., 2018). Moho depth increases gradually southwards from 17 km to 31 km across the North Africa margin (Figure 4a).

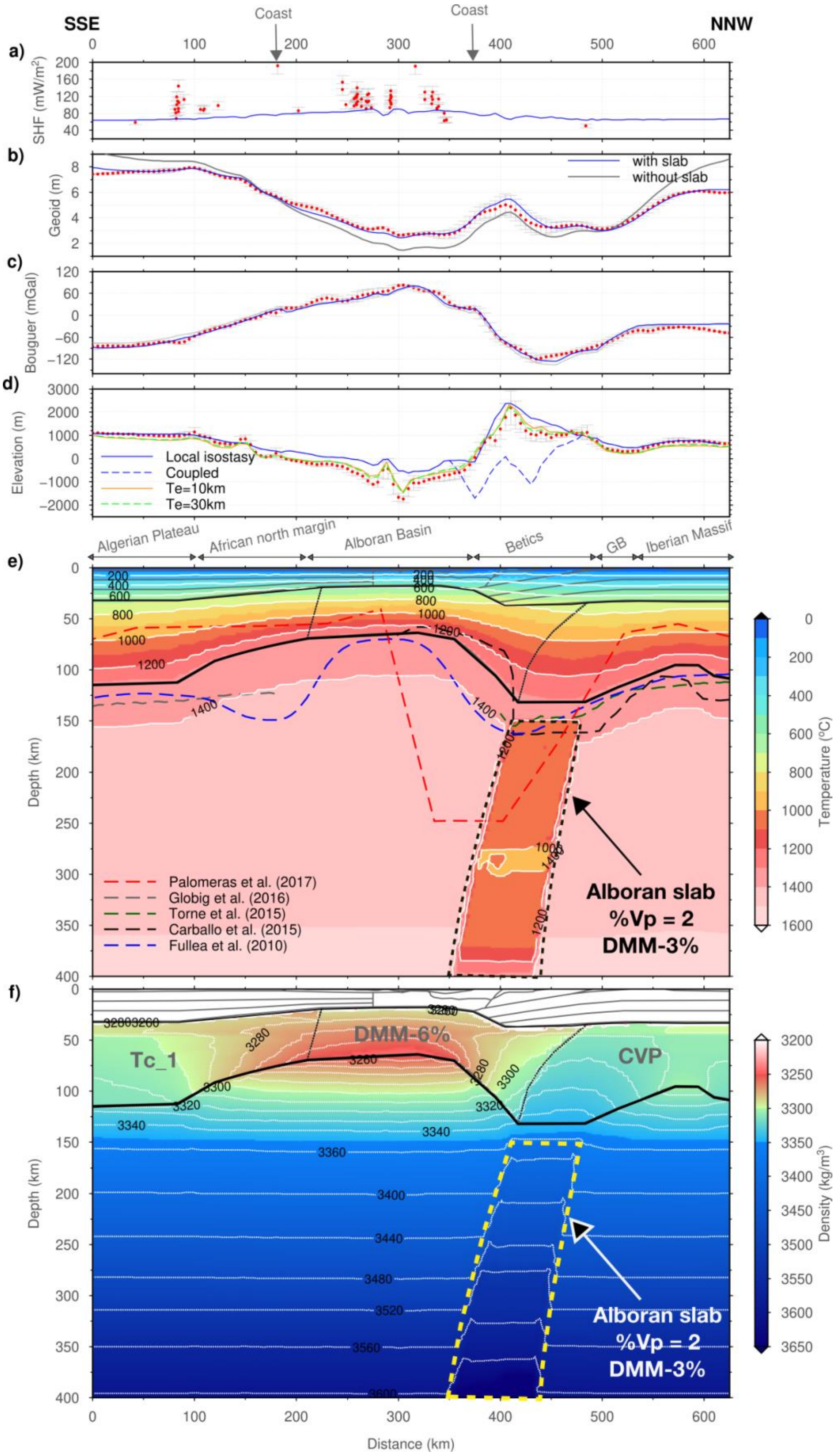
SSE
NNW
Coast
Coast
a)
SHF (mW/m^2)
b)
Geoid (m)
with slab
without slab
c)
Bouguer (mGal)
d)
Elevation (m)
Local isostasy
Coupled
Te=10km
Te=30km
Algerian Plateau
African north margin
Alboran Basin
Betics
GB
Iberian Massif
e)
Depth (km)
Palomeras et al. (2017)
Globig et al. (2016)
Torne et al. (2015)
Carballo et al. (2015)
Fullea et al. (2010)
Alboran slab
%Vp = 2
DMM-3%
Temperature (ºC)
f)
Tc_1
DMM-6%
CVP
Depth (km)
Alboran slab
%Vp = 2
DMM-3%
Density (kg/m^3)
Distance (km)

Figure 5. Best fitting model along the Alboran Basin geo-transect. (a) Surface heat flow. (b) Geoid height. (c) Bouguer anomaly. (d) Elevation. Blue line shows the calculated values from the model. Red dots denote measured data, and vertical bars denote the standard deviation calculated across a strip of 25 km half width. In (b) geoid height with no slab anomaly is plotted in grey for comparison. In (d) isostatic elevation is plotted in solid blue while the effect of slab on elevation (coupled elevation) is plotted in dashed blue line. Elevation assuming flexural isostasy for elastic thickness of 10 km and 30 km are plotted in orange and light-green, respectively. (e) Temperature distribution along the geo-transect. Continuous black lines highlight the Moho and LAB depth from our model. LAB depths from previous studies (dashed color lines) are overlay for comparison. (f) Density distribution in the mantle. The different composition domains in the lithospheric mantle, indicated by codes listed in Table 2, are separated by thin dotted-black lines.

We have deemed three different chemical composition domains within the lithospheric mantle (Table 2 and Figure 5) along the Alboran Basin geo-transect. For the Iberian lithosphere, we have considered a depleted composition taken from mantle xenoliths sampled in the Calatrava Volcanic Province (CVP, Villaseca et al., 2010) as in Jiménez-Munt et al. (2019). In the Alboran Basin, the lithospheric mantle composition corresponds to the residual of 6% aggregate decompressional melting of DMM based on the pervasive magmatic intrusion related to the retreat of the Tethyan slab named as Alboran slab throughout the paper. This chemical domain extends beneath the Betic orogenic system as a result of the NNW directed slab roll-back and associated mantle delamination (Figure 5, see discussion). In the North African margin and the Algerian Plateau, the composition of the lithospheric mantle corresponds to Average-Garnet-Tecton, an average Phanerozoic mantle composition (Tc_1; Griffin et al., 2009), in agreement with previous models of the region (e.g., Fullea et al., 2010; Carballo et al., 2015a). The LAB depth is ~110 km beneath the stable Iberian Massif increasing to ~130 km beneath the Betics and rising abruptly to ~60 km towards the Alboran Basin from where the LAB deepens gently beneath the North African margin down to ~112 km below the Algerian Plateau (Figure 5e).

Seismic tomography models show a positive P-wave velocity anomaly beneath the Betics that amounts ~1–3 % relative to the ak135 global velocity model (e.g., Garcia-Castellanos and Villaseñor, 2011; Bezada et al., 2013; Villaseñor et al., 2015) and an excess of 0.15–0.3 km/s in S-wave velocity (e.g., Palomeras et al., 2014, 2017; Civiero et al., 2018). This anomaly extends down to 670 km depth and has been interpreted as the Ligurian-Tethys subducted lithosphere that is detached from the Iberian lithosphere along a lateral tear affecting the region crossed by the geo-transect (e.g., Spakman and Wortel, 2004; Garcia-Castellanos and Villaseñor, 2011; Bezada et al., 2013; Palomeras et al., 2017) (Figures 2b and 2c). Consequently, we have considered a sublithospheric mantle anomaly situated below 140 km depth simulating the detached Alboran slab characterized by a P-wave velocity anomaly of ΔV_P = 2% and using the residual composition after 3% aggregate melting from DMM (DMM-3%; Figure 5e). We have tested different possible chemical compositions for the slab ranging from pure oceanic lithosphere to CVP, DMM-3% being the one with the best-fitting (Table 3 and Figure S2).

Table 3. Root mean square error (RMSE) associated with the tested models in the Alboran Basin geo-transect. To calculate the RMSE related to geoid, gravity and elevation we have considered the absolute difference (error) between the calculated and observed values and its associated standard deviation. Therefore, error = 0, for |*calc* - *obs*| ≤ *std*, and error = |*calc* - *obs*| - *std*, for |*cal* - *obs*| > *std*; where *calc*, *obs*, and *std* are the calculated and observed values, and the standard deviation, respectively. Note that for the models with slab, elevation corresponding to Te=0 km is calculated assuming that the slabs are not attached with the lithosphere.

Model	**Model fit (RMSE)**				
	Geoid (m)	**Bouguer anomaly** (mGal)	**Elevation** (m)		
			Te=0km	**Te=10km**	**Te=30km**
homogenous lithospheric mantle composition (Tc_1)	0.96	12.41	332	96	73
without the slab	0.85	7.41	256	62	42
Alboran slab with DMM-3% composition (Figure 5)	0.10	5.26	552	266	164
Alboran slab with DMM-7% Composition	0.20	5.42	415	197	113
Alboran slab with CVP composition	0.31	5.55	1058	500	339

Table 3 displays the root mean square error (RMSE) associated with different tested models including homogenous lithospheric mantle composition, no slab, detached slab of different compositions (CVP, DMM-3% and DMM-7%; Table 2), and different elastic thickness (Te = 0 km, 10 km and 30 km). Fit to the surface observables increase on considering three different composition domains in the lithosphere along the Alboran Basin geo-transect. Variations in the composition of the detached slab decrease noticeably the RMSE of the geoid height and in a lesser extent the RSME of the Bouguer gravity anomaly. If the sublithospheric anomaly is ignored, the RMSE related to the geoid height is eight times higher and then is unacceptable as shown in Figure 5b. Variations in RMSE of the elevation are due to the density variations associated with slab composition and resulting pressure variations related to topography loads at the base of the model.

The geophysical observables and the calculated values obtained with the proposed model are shown in the upper panels of Figure 5. The calculated SHF falls within the available measurements, though these are sparse and uncorrected for surface perturbations and transient effects (Figure 5a). Deep groundwater circulation in the Tell Mountains can result in anomalously high heat flow in the Algerian Plateau. Similarly, recent mantle upwelling and volcanism can be responsible for the high heat flow measured in the Alboran Basin. The calculated geoid height and the Bouguer gravity anomaly match satisfactorily the observations (Figures 5b and 5c), whereas local isostatic elevation shows remarkable misfits of ~100 m in the Guadalquivir basin, and ~500 m in the Betics and the Alboran Basin (Figure 5d). However, when flexural rigidity of the lithosphere is considered and vertical loads associated with the topography misfits are applied, the calculated elevation fits well with the observations (Fig. 5d). An effective elastic thickness of 10 km is enough to fit the elevation over most of the geo-transect, this value agrees with the elastic thickness obtained in the same region from other methodologies (e.g. Kaban et al., 2018). It is worth noting that elevation is well reproduced when considering that the sublithospheric anomaly related to the detached slab does not transfer any traction stress on the overlying lithosphere, i.e. it is mechanically decoupled (Figures 5d and S4a). In the case that the slab would transfer all the gravitational potential to the surface, i.e. when the sublithospheric anomaly is fully coupled to the lithosphere, the resulting isostatic elevation would decrease by ~1000–2000 m in the Betic region and increase by few hundred meters in the Alboran Basin depending on the considered equivalent elastic thickness (dashed lines in Figure S4a).

5.1.2 Temperature and density distribution

The temperature distribution along the entire geo-transect is shown in Figure 5e. The Iberian Massif is characterized by flat isotherms in the crust with a Moho temperature of ~650 °C, and a slight upward deflection at deep lithospheric mantle levels related to the thinning of the lithosphere beneath the Calatrava Volcanic Province. In the Betics, the deepening of the LAB produces the downward deflection of the isotherms. The maximum Moho temperature along the geo-transect is reached in the Betics (800 ºC) as a combined effect of crustal thickening and the sharp lithospheric thinning towards the adjacent Alboran Basin, where Moho temperatures are around 550 ºC. Towards the stable Algerian Plateau the isotherms become roughly horizontal with a Moho temperature similar to the Iberian Massif (~650 ºC). The temperature distribution within the sublithospheric mantle results from the combined effect of lithospheric thickness variations and the imposed adiabatic thermal gradient except within the detached lithospheric slab where the input P-wave velocity anomaly of ΔV_P = +2% translates into a temperature anomaly of $\Delta T \approx$ -430 ºC (Figures 5e and S5). The calculated density variations in the lithospheric mantle are due to the different chemical compositions and the P-T conditions resulting from laterally varying the lithospheric thickness (Figure 5f). In the Iberian Massif, density is almost constant in the Calatrava Volcanic Province (3300–3310 kg/m^3) increasing rapidly towards the Betics where density increases with depth from 3300 kg/m^3 beneath the Moho to ~3350 kg/m^3 near the LAB. This lateral change in the density distribution is mainly related to the variations in the LAB depth and its effect on pressure and temperature distribution. The pronounced lithospheric thinning affecting the Alboran Basin results in high temperature and low pressure conditions that decrease the density in the lithospheric mantle. This effect adds to the density decrease associated with the compositional change between the Iberian lithospheric mantle (CVP) to the oceanic-like lithospheric mantle of the Alboran basin (DMM-6%), which may amount 10–15 kg/m^3 (Table 2). As a result, the lithospheric mantle density in the central part of the Alboran Basin shows the lowest values along the geo-transect with a depth-dependent decrease from 3290 kg/m^3 beneath the Moho to 3250 kg/m^3 near the LAB. Towards the Iberian and African margins density increases laterally and keeps almost constant with depth due to strong variations in the LAB depth indicating that in these regions pressure and temperature effects tend to counterbalance each other. Beneath the stable Algerian Plateau density in the lithospheric mantle increases with depth from 3270 kg/m^3 to 3320 kg/m^3.

At shallow sublithospheric mantle levels, the lateral density variations are related to changes in the lithospheric thickness such that the thinner the lithosphere the lower the density, with values ranging from 3345 kg/m^3 beneath the Betics to 3260 kg/m^3 beneath the Alboran Basin. At deeper sublithospheric mantle depths (>150 km) density increases with depth almost linearly and lateral variations are negligible, except for the cold and detached Alboran slab region, where the associated density anomaly amounts ~50 kg/m^3 and increase by ~125 kg/m^3 at the base of the model (400 km) due to the depth decrease of the olivine-wadsleyite phase transition resulting from the colder temperatures within the slab (Figures 5 and S5).

5.2 The Algerian Basin geo-transect: structure, temperature, and density

5.2.1 Crustal and upper mantle structure

The crustal structure roughly coincides with that proposed by Carballo et al. (2015a) except for the three-layered continental crust and the internal structure of the Greater Kabylies (Figure 4b). The crust is ~36 km thick beneath the Tell-Atlas Mountains gently thinning towards the margin up to ~30 km with the basement deepening smoothly beneath the Greater Kabylies. The Greater Kabylies are characterized by high density metamorphic slices (Internal Units) thrusting onto the folded non-metamorphic Mesozoic External Units overlying the African crust showing a similar architecture to the Betics (Figure 4a). Further to the NNW, the crust thins abruptly towards the Algerian Basin where the Moho is found at 10–12 km depth. The crust of the Algerian Basin is composed of a ~6 km thick oceanic layer overlaid by a ~3 km thick Neogene sedimentary layer. The Balearic Promontory, the Valencia Trough and the Catalan Coastal Ranges are characterized by a thinned continental crust and a Mesozoic to Neogene sedimentary cover of variable thickness. Our results are consistent with previous findings derived from active seismic experiments (e.g., Torne et al., 1992; Vidal et al., 1996) who proposed a clear crustal asymmetry across the Trough, with thickness of ~32 km underneath the Iberian margin, and a thinner crust (~22 km) below the Balearic Promontory. In the axis of the Valencia Trough the Moho is found at ~18 km along the modeled geo-transect, in agreement with the aforementioned works (Figure 4b).

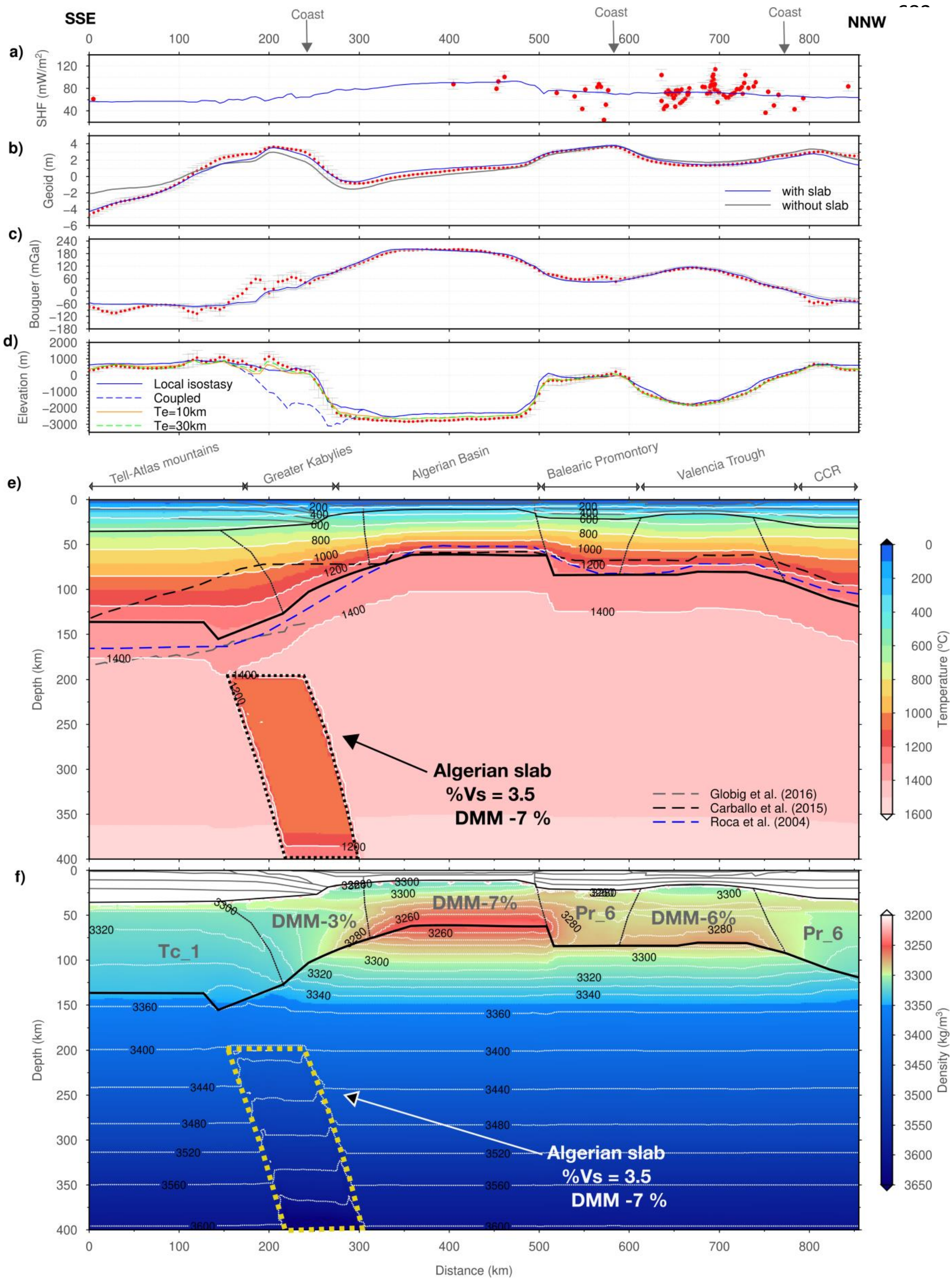

Figure 6. Best fitting model along the Algerian basin geo-transect. Figure caption same as in Figure 5.

Along the Algerian Basin geo-transect, we have considered five lithospheric mantle domains (Figure 6 and Table 2) following the structure from Carballo et al. (2015a) and considering the different tectonic domains. In the Catalan Coastal Ranges and the Balearic Promontory, we use an Average Proton Lherzolite (Pr_6; Le Roux et al., 2007; Griffin et al., 2009), as in Carballo et al. (2015a) except for the Balearic Promontory where they used a primitive upper mantle composition. In the Valencia Trough, we use a residual composition corresponding to DMM-6% based on the inferred high degree decompression melting driven by lithospheric extension and mantle upwelling (Martí et al., 1992). Since, the Algerian Basin is a back-arc oceanic basin with a ~6 km thick oceanic magmatic layer (Booth-Rea et al., 2007), we have increased the amount of melting to ~7% (Klein and Langmuir, 1987), while beneath the Greater Kabylies this percentage is reduced to 3% to account for the melting of the depleted asthenosphere (DMM) following delamination and slab detachment (Chazot et al., 2017). In the North Africa margin, beneath the Tell-Atlas Mountains, we have deemed a lithospheric mantle with a Phanerozoic Tc_1 composition according to Carballo et al. (2015a). Using different composition domains in the lithospheric mantle increases fit to the surface observables as opposed to the model with homogenous lithospheric mantle composition (Table 4). The LAB depth varies from ~135 km over a flat region beneath the Tell-Atlas Mountains to ~150 km below the Greater Kabylies and decreases rapidly to ~60 km in the Algerian Basin. Towards the Balearic Promontory, the LAB deepens abruptly to ~84 km and shallows slightly towards the centre of the Valencia Trough (~80 km) and increases gradually to ~120 km onshore Iberia.

The positive seismic velocity anomaly beneath the Kabylies-Tell orogenic system (Figure 2d; after Fichtner and Villaseñor, 2015) is interpreted as a detached Ligurian-Tethys slab, hereinafter named as Algerian slab. The modeled Algerian slab is situated below 200 km depth with an anomalous S-wave velocity of $\Delta V_S = +3.5\%$ and a chemical composition similar to that of the present-day Algerian Basin lithospheric mantle (DMM-7%). This composition fits better the geoid height than the more enriched DMM-3% considered for the delaminated mantle beneath the Greater Kabylies (Table 4 and Figure S3).

Table 4. Root mean square error (RMSE) associated with the tested models for the Algerian Basin geo-transect. Table caption same as in Table 3.

Model	**Model fit (RMSE)**				
	Geoid (m)	**Bouguer anomaly** (mGal)	**Elevation** (m)		
			Te=0km	**Te=10km**	**Te=30km**
homogenous lithospheric mantle composition (Tc_1)	0.78	15.17	226	48	31
without the slab	0.56	14.8	202	52	30
Algerian slab with DMM-3% composition	0.36	12.85	723	285	214
Algerian slab with DMM-7% composition (Figure 7)	0.25	13.14	535	212	153

Figure 6 shows the fit to the geophysical observables from the proposed model. The calculated SHF falls within the range of measured values though these are unevenly distributed and show a high scatter (Figure 6a). The calculated geoid height shows a very good fit with observations all along the geo-transect (Figure 6b), with minor misfits (< 1 m) in the Greater Kabylies. The calculated Bouguer anomaly matches the regional trend (Figure 6c) with significant misfits all along the Greater Kabylies, where the calculated values are clearly underestimated probably due to the little gravity data available in the region. The best fitting model shows the minimum estimated RMSE values for geoid height and Bouguer anomaly, 0.25 m and 13.14 mGal, respectively, when compared to a no slab model or to a model with DMM-3% slab composition (Table 4 and Figure S3).

The calculated isostatic elevation also matches the regional trend but shows long wavelength misfits of ~400 m in the Algerian Basin and ~250 m in the Tell-Atlas Mountains, with local misfits of ~700 m in the Greater Kabylies (Figure 6d). However, when we consider the flexural rigidity of the lithosphere, the fit between calculated and observed elevation is largely improved (Figure 6d). Along most of the profile, an effective elastic thickness of Te = 10 km reduces the RMSE from 202 m to 52 m (Table 4), although a higher elastic thickness (Te = 30 km) is required for the Africa mainland resulting in RMSE = 30 m (Figure S4b and Table 4). These elastic thickness values are in agreement with those predicted by coherence analysis of topography and gravity (e.g., Pérez-Gussinyé et al., 2009; Kaban et al., 2018). The estimated coupled elevation, which includes the isostatic effect of the cold and denser slab, would decrease the elevation by ~500–2000 m in the Greater Kabylies and by few 100 m in the Algerian Basin close to the coast, and increase by few 100 m further to the NNW depending on the elastic thickness (Figures 6d and S4b).

5.2.2 Temperature and density distribution

The temperature distribution along the Algerian Basin geo-transect is shown in Figure 6e. At deep lithospheric levels, isotherms mimic the depth variations of the LAB showing a step-like shape. In the Tell-Atlas Mountains region, isotherms are roughly flat showing an upward deflection beneath the Great Kabylies and the Africa margin, and become flat again in the Algerian Basin. Further to the NNW, isotherms deepen slightly below the Balearic Promontory flattening beneath the Valencia Trough and deepening gently towards the Catalan Coastal Ranges. The calculated temperature at the Moho varies from ~630 ^{o}C in the Tell-Atlas Mountains, decreasing rapidly beneath the Greater Kabylies (600–400 ^{o}C) and reaching the minimum value of ~250 ^{o}C in the Algerian Basin. Towards the Iberia Margin, the Moho temperature shows noticeable variations reaching ~600 ^{o}C in the Balearic Promontory, ~400 ^{o}C in the Valencia Trough and ~700 ^{o}C in the Catalan Coastal Ranges. At sublithospheric mantle levels, below 200 km depth, the temperature distribution responds to the imposed adiabatic thermal gradient except within the detached Algerian slab, where the input seismic anomaly of ΔV_S = 3.5% translates into a temperature anomaly of $\Delta T \approx$ -400 ^{o}C (Figures 6e and S6).

The calculated density distribution along the Algerian Basin geo-transect is shown in Figure 6f, and reflects the different chemical compositions and pressure-temperature conditions in the upper mantle. The lithospheric mantle in the Tell-Atlas Mountains, with the same composition than in the Algerian Plateau from the Alboran

Basin geo-transect (i.e., Tc_1, Table 2) shows a density increase with depth from ~3280 kg/m^3 at the Moho to ~3340 kg/m^3 at the LAB. It is slightly higher than in the Algerian Plateau lithosphere of the parallel Alboran Basin geo-transect (3270–3320 kg/m^3, respectively, Figure 5f) due to the deeper LAB. Density decreases laterally across the margin, beneath the Greater Kabylies, and towards the Algerian Basin from 3320 kg/m^3 to less than 3290 kg/m^3, being almost constant with depth. These density changes are the combined effect of varying the chemical composition from Tc_1 to DMM-3% (Table 2) and the lithospheric thinning, which counterbalances the depth-dependent pressure and temperature effects. The oceanic lithospheric mantle in the Algerian Basin, with a DMM-7% composition (Table 2), shows a density exceeding 3300 kg/m^3 at the uppermost mantle levels until a depth of ~20 km related to the plagioclase-spinel phase transition. Below this depth, density decreases with depth to 3250 kg/m^3 at the LAB, which is the lowest mantle density along the geo-transect. To the NNW, the transition to a Proterozoic composition (Pr-6, Table 2) beneath the Balearic Promontory together with the lithosphere thickening, results in a lateral increase of densities to an average value of ~3285 kg/m^3 which keeps almost constant with depth. The lithospheric mantle beneath the Valencia Trough, with DMM-6% composition, shows a density of ~3300 kg/m^3 at the Moho depth decreasing to 3280 kg/m^3 at the LAB, demonstrating some oscillations in the pressure gradient related to the plagioclase-spinel (25–35 km depth) and spinel-garnet (60–90 km depth) phase transitions. Density increases again laterally towards the Catalan Coastal Ranges as a combined effect of composition and pressure-temperature conditions. Similar to the Alboran Basin geo-transect, at shallow sublithospheric mantle levels, density variations are related to LAB depth variations affecting especially the Algerian Basin, the Balearic Promontory, and the Valencia Trough regions. At deeper sublithospheric mantle levels (>150 km), lateral variations are negligible, except for the detached Algerian slab region where density increases by ~30 kg/m^3 up to ~300 km depth and decrease to < 20 kg/m^3 at 350 km depth as pressure and composition effects competes with those of temperature (Figure S6). Note that the slab has the same composition as the present-day oceanic lithosphere in the Algerian Basin (i.e., DMM-7%, Table 2). Close to the base of the model, density increases by as much as ~100 kg/m^3 in the slab region due to the olivine-wadsleyite phase transition alike to the Alboran slab at these depths (Figures 6 and S6).

5.3 Mantle seismic velocities

In this section, we show the calculated seismic velocities in the upper mantle according to the stable mineral aggregates resulting from the ascribed chemical composition and the prevailing pressure and temperature conditions. The results are compared with available seismic velocities and tomography models.

5.3.1 Alboran Basin geo-transect

Figure 7a shows the P-wave velocity distribution along the Alboran Basin geo-transect. As shown in Table 2, seismic velocities depend to a larger extent on temperature and pressure than on composition. The lower V_P values within the lithospheric mantle are found close to the LAB in regions affected by lithospheric thinning, as the Calatrava Volcanic Province in the Iberian Massif ($V_P < 8.0$ km/s), and the Alboran Basin and its margins ($V_P < 7.85$ km/s). In these regions, V_P decreases with depth indicating that the temperature effect prevails on the pressure effect. In contrast, P-wave velocities beneath the Betics, in the thicker lithosphere region, increase from ~8.05 km/s in the uppermost mantle, consistent with the observed P_n velocities of 8.0–8.2 km/s (Diaz et al., 2009, 2013), to 8.1 km/s at LAB depths. Beneath the Algerian Plateau, P-wave velocities keep almost constant with depth ($V_P \approx 8.0$ km/s) showing a lateral decrease towards the Africa margin.

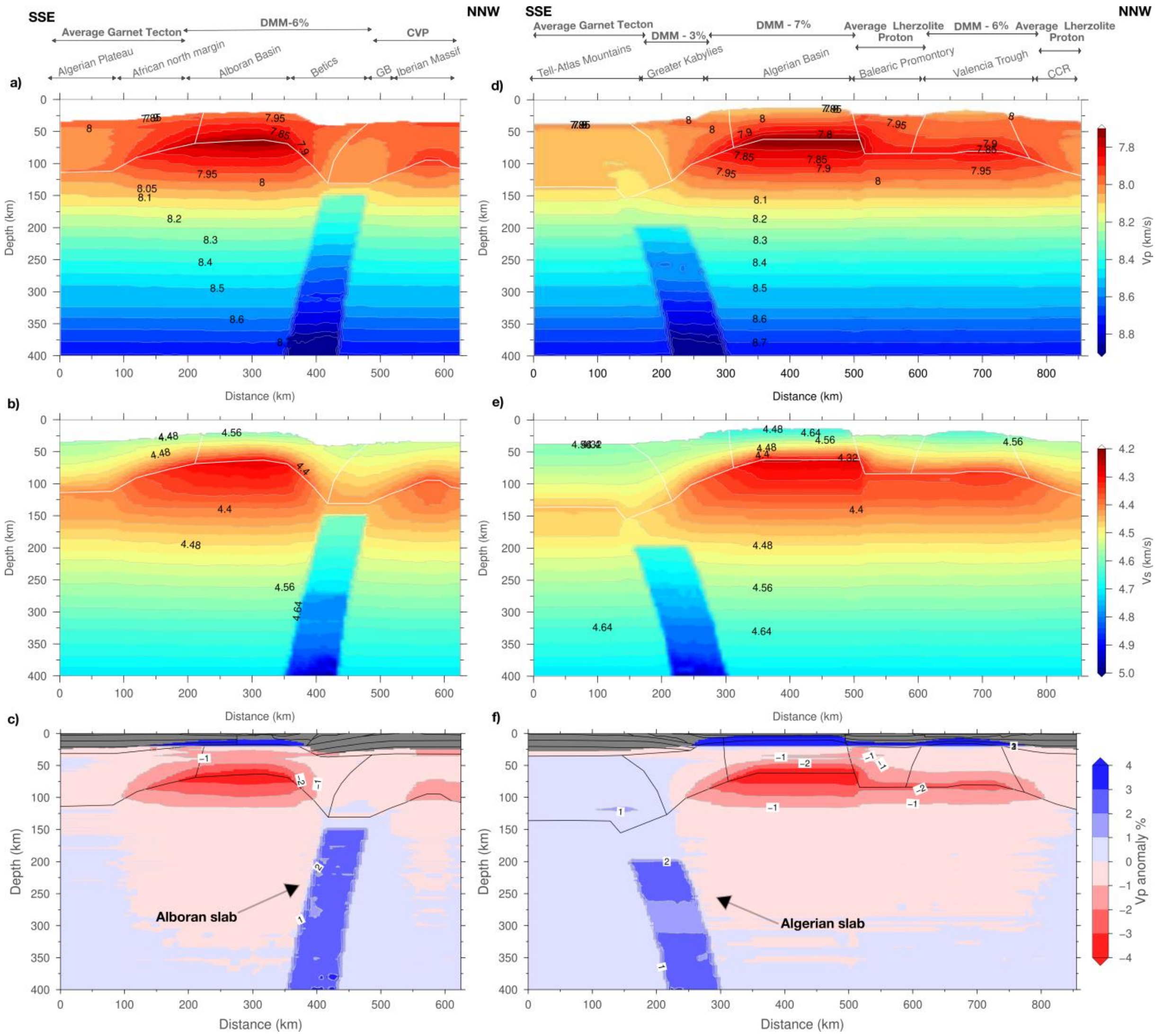

Figure 7. Seismic velocities and synthetic seismic tomography along the geo-transects. (a) and (b) show absolute P- and S-wave velocities, respectively and (c) synthetic P-wave anomalies for the Alboran Basin geo-transect. Similarly, (d) and (e) show absolute P- and S-wave velocities, respectively, and (f) P-wave anomalies for the Algerian Basin geo-transect.

The relatively fertile (DMM-6%) composition of the central segment of the geo-transect, close to primitive upper mantle (PUM; McDonough and Sun, 1995), produces shallow mantle P-wave velocities of 7.97 km/s in the Alboran Basin as found by Fullea et al. (2010). These low P-wave velocities can be further reduced by the presence of partial melts, as the geotherm intersects the peridotite solidus (Figure S7), and anisotropy (not considered here) becoming close to the observed low P_n velocities (7.5–8.1 km/s, Hatzfeld et al., 1978; Calvert et al., 2000) and upper mantle velocity of ~7.9 km/s beneath the East Alboran Basin (Gómez de la Peña et al., 2020). At sublithospheric mantle depths down to 150 km, lateral variations of seismic velocities result solely from the pressure-temperature conditions imposed by the lateral lithospheric thickness variations since the entire sublithospheric mantle has the same composition, except in the slab region. Below 150 km, P-wave velocities increase almost linearly with depth up to > 8.7 km/s at 400 km depth. In the region of the detached Alboran slab, P-wave velocities increase by ~0.18 km/s as imposed from tomography models (ΔV_P = 2%) with a highest increase of ~0.30 km/s just above 400 km depth related to the olivine-wadsleyite phase transition (Figures 7a and S5).

Calculated S-wave velocities (Figure 7b) show a similar pattern than P-wave velocities but with a lesser influence of pressure, such that V_S decreases with depth from Moho to LAB all along the geo-transect. Likewise, laterally varying compositional domains show smaller effects on V_S than on V_P due to the lesser sensitivity of S-wave to composition (e.g., Priestley and McKenzie, 2006; Kumar et al., 2020). Below the LAB, V_S increases with depth delineating a low-velocity zone down to 200–250 km which is enhanced in magnitude in those regions affected by lithospheric thinning. The Alboran slab shows an S-wave velocity increase of ~0.15 km/s (+3.5%) resulting from the prescribed P-wave anomaly. The calculated S-wave velocity pattern compares well with the regional S-wave tomography model projected onto the transect (Figure 2c) obtained by Palomeras et al. (2017) from Rayleigh surface-wave dispersion tomography.

In order to compare the computed mantle velocities with the P-wave travel-time tomography models, the lateral variations of P-wave in % are calculated relative to the reference column defined in LitMod2D_2.0, with a 35 km crust and lithospheric mantle of Tc_1 composition and LAB at 120 km (Kumar et al., 2020) (Figure 7c). The computed synthetic tomography reproduces the main pattern of slow and fast velocity regions observed in the global/regional P-wave tomography models (Bezada et al., 2013, Figure 2b) with minor discrepancies in the amplitudes. Note that the color scale of the calculated tomography saturates in the regions with Moho depth < 35 km because of the used reference model, which consists of a 35 km crust (Kumar et al., 2020) and highlights the crustal thinning as observed in the tomography model of Bezada et al. (2013)(Figure 2b).

5.3.2 Algerian Basin geo-transect

Figure 7d shows the calculated P-wave mantle velocities along the Algerian Basin geo-transect. As in the Alboran Basin geo-transect, the lower velocities are found at LAB levels in regions affected by lithospheric thinning including the Algerian Basin, the Balearic Promontory and the Valencia Trough. In these regions, V_P decreases from 7.90–7.95 km/s beneath the Moho to < 7.9 km/s at LAB depths with the lowest value along the whole geo-transect (< 7.8 km/s) being at the Algerian Basin. The calculated uppermost mantle velocities are slightly higher than the reported P_n velocities in the Valencia Trough and the Algerian Basin, ranging from 7.7 km/s to 7.95 km/s (Dañobeitia et al., 1992; Torne et al., 1992; Vidal et al., 1998). Towards the Iberian and African margins (Catalan Coastal Ranges and Greater Kabylies, respectively), P-wave velocities increase laterally showing almost constant values with depth. Beneath the thicker lithosphere of the Tell-Atlas Mountains, P-wave velocities increase with depth from 7.9 km/s at the Moho to 8.1 km/s at the LAB, being slightly higher than in the Algerian Plateau lithosphere (Figure 7a). Down to ~150 km depth, the effect of lithosphere thickness is reflected in P-wave velocities, where the thin lithosphere of the Algerian Basin results in a low velocity zone, similar to that in the Alboran Basin, extending towards the Balearic Promontory and the Valencia Trough. Below 150 km, P-wave velocities are essentially depending on pressure increasing mostly linearly with depth up to >8.7 km/s at 400 km depth. In the region of the detached Algerian slab, P-wave velocities are increased by ~0.18 km/s (~2%) and near the base of the slab (400 km) increase by ~0.30 km/s (> 3%) because of the olivine-wadsleyite phase transition (Figures 7d and S6).

S-wave velocities also show a low velocity zone extending from mid-lithospheric mantle levels to 200–250 km depth being more pronounced beneath the Algerian Basin, the Balearic Promontory and the Valencia Trough due to the prevalence of temperature effects on pressure effects in these regions (Figure 7e). Minimum values of S-wave velocities (≤ 4.35 km/s) are obtained at the base of the lithosphere along the thinned lithosphere regions, whereas beneath the Africa and

Iberia mainland minimum S-wave velocities exceed 4.45 km/s. The region corresponding to the detached Algerian slab, is characterized by an average increase of S-wave velocity of ~0.16 km/s in agreement with the prescribed anomaly of $\Delta V_S = 3.5\%$.

The computed synthetic P-wave tomography (Figure 7f) shows negative V_P anomalies of less than -2% beneath the Algerian Basin and the Valencia Trough in agreement to regional and global P-wave tomography models (e.g., Piromallo and Morelli, 2003; Spakman and Wortel, 2004; Amaru, 2007). The detached Algerian slab is characterized by a positive V_P anomaly ~2% resulting from the prescribed V_S anomaly ($\Delta V_S = 3.5\%$; Fichtner and Villaseñor, 2015).

6. Discussion

6.1 Crustal and lithospheric structure

The multiple seismic surveys carried out in the study region allows us to have a good constraint on the Moho depth along most of the Alboran and Algerian basins geo-transects (Figure 4). The regions that are less constrained are the Algerian Plateau, the Tell-Atlas Mountains and the Greater Kabylies where deep seismic data are not available. We have considered that the crust of the Iberia and Africa mainland along both geo-transects consists of three layers, namely upper, middle and lower crust, plus a sedimentary cover. The geometry of these crustal layers responds to the density variations required to fit the observables (Bouguer anomaly, geoid, and elevation) and to tectonic criteria.

The structure of the Internal Betics and Greater Kabylies is more complex and differs noticeably from previous lithospheric cross-sections (e.g., Frizon de Lamotte et al., 2004; Roca et al., 2004; Carballo et al., 2015a and b). In these regions, we have included exhumed high-density metamorphic rocks of the Internal Units overthrusting the folded External Units that belonged to the former passive margins of Iberia and northern Africa (See *Geodynamic implications,* section 6.3). Across the Alboran Basin, main differences with previous transects are due to the incorporation of recent interpretations of seismic data that led us to consider a thin and highly intruded continental crust in the North Alboran Basin transitioning to a magmatic crust in its central part (Gómez de la Peña et al., 2018). Seismic data suggests a noticeable transition in the centre of the Alboran Basin (Alboran Ridge; Figure 2a) separating the magmatic crust domain from the thinned North-Africa continental crustal domain in the South Alboran Basin (Martínez-García et al., 2017), transitioning southwards to the thicker African crust. With this crustal configuration, the Moho depth obtained from our models is generally within the uncertainty bounds of seismic data and follows similar trends of previous studies with some localized differences in the margins of the Alboran and Algerian basins and the Valencia Trough (Figure 4). Indeed, noticeable discrepancies on Moho depths derived from receiver functions (Diaz et al., 2016) are observed beneath the Betics, which can be attributed to the presence of intra-crustal dipping layers with varying V_P/V_S ratio, and to a heterogeneous crustal structure.

Figures 5e and 6e compare the calculated LAB depths to that reported from other modeling approaches and techniques showing that although there is coincidence with the main trends of lithospheric thickness variations, there are also pronounced discrepancies. Along the Alboran Basin geo-transect, the LAB depth beneath the Iberian Massif, the Betics Mountains and the North Alboran Basin is consistent with previous models based on potential field modeling and thermal analysis (Torne et al., 2015) and 2D geophysical-petrological modeling (Carballo et al., 2015b), though our LAB depth values are consistently shallower. These discrepancies in LAB depth (< 15%) are related to the different modeling approach and the simplified crustal structure used in Torne et al. (2015), and the differences in the geometry of intra-crustal bodies beneath the Betics and the chemical composition of the sublithospheric mantle used in Carballo et al. (2015b).

Discrepancies with the LAB depth derived from the 3D geophysical-petrological model by Fullea et al. (2010) are noticeably larger (Figure 5e). The LAB proposed by Fullea et al. (2010) beneath the Betics and the North-African margin is significantly deeper than ours, with a similar lithospheric thinning below the Alboran Basin affecting a narrower region. These discrepancies maybe related to the simpler crustal structure considered by these authors, differences in crustal thickness and chemical compositional domains in the Alboran Basin lithosphere (PUM instead of DMM-6%) and sublithospheric mantle (PUM instead of DMM), and lack of the radiative contribution in calculating the mantle thermal conductivities. The LAB depth beneath the North-African margin derived from combined elevation and geoid modeling by Globig et al. (2016) is also noticeably higher (Figure 5e) due to the different approach used by these authors, yielding a > 5 km thicker crust in this region (Figure 4a).

The LAB depth proposed by Palomeras et al. (2017) shows a similar lateral trend with consistently shallower depths that roughly follows the 1000 ± 50ºC isotherm, except beneath the Betics where the LAB is deeper coinciding with the positive velocity anomaly related to the Alboran slab (Figure 5e). Seismically, the LAB is defined as a low-velocity layer and is derived from the depth of the negative S-wave velocity gradient obtained from surface waves and therefore, is a proxy of the base of the high-velocity mantle lid (Palomeras et al., 2017). A major misfit occurs at the central part of the Alboran Basin where the seismically derived LAB is at 250 km depth. Although the precise determination of the LAB depth depends on how it is measured (Eaton et al., 2009), the different definitions should show a similar trend as they all are imaging the rheological strong outer layer of the Earth.

Along the Algerian Basin geo-transect, the previous studies extending along the whole profile are from Roca et al. (2004), based on a pure-thermal integrated geophysical approach with a temperature-dependent lithospheric mantle density, and Carballo et al. (2015a), based on an integrated geophysical-petrological methodology. Both show similar results from the Catalan Coastal Ranges to the southern margin of the Algerian Basin, which are also roughly coincident with our study despite the methodological differences (Figure 6e). It is worth noting that beneath the Algerian margin and the Greater Kabylies none of the previous studies, including Globig et al. (2016), considered the presence of a detached Ligurian-Tethys slab segment (Figure 2d). Despite of that, main discrepancies are found regarding to the work by Carballo et al. (2015a), who proposed a LAB depth up to 60 km shallower than in our work beneath the Greater Kabylies, whereas discrepancies with Roca et al. (2004) and Globig et al. (2016) amount less than 20–25 km. The method used in Carballo et al. (2015a) is similar to our approach; except that these authors do not consider the radiation contribution in the calculation of mantle thermal conductivity. Therefore, differences in the LAB-depths can be mainly attributed to small differences in the calculated mantle thermal conductivity, but also to the crustal structure (Figure 4b) and to the positive seismic velocity anomaly associated with the Algerian slab, resulting in a deeper LAB in this part of the geo-transect (Figure 2d).

6.2 Mantle composition and subducted Ligurian-Tethys slabs

Identifying bulk mantle composition based on density and seismic velocities is not straightforward because of the highly non-linear nature of the problem and the non-uniqueness. Based on a non-linear 3D multi-observable probabilistic (Bayesian) inversion, Afonso et al. (2013a and b) show that a wide range of compositions can, equally well, explain multiple geophysical data. In consequence, the considered mantle chemical compositions compatible with the geophysical observables needs further appraisal based on the geological history. Our main aim is to compare the structure of the Betics and Kabylies-Tell orogens and the associated Alboran and Algerian back-arc basins, and the mantle composition.

Although there is no univocal relationship between mantle chemical composition and its density and elastic properties, we can relate the considered lithospheric mantle composition to major geodynamic processes operating in the Western Mediterranean, which are dominated by subduction of the Ligurian-Tethys Ocean. Subduction processes can modify mantle composition by incorporating fluids and sediments carried by the subducting slab resulting in chemical enrichment by metasomatism (Ringwood, 1974; Spandler and Pirard, 2013). At the same time, mantle flow generated during subduction can produce melting by adiabatic decompression, which will deplete the sublithospheric mantle (Magni, 2019). Generally, volcanic rocks produced from mantle melting show geochemical signatures similar to the environment in which they are produced. However, interactions of magmas with crustal rocks during its ascent and emplacement can influence their geochemical signature. Melchiorre et al. (2017), using Principal Component Analysis (PCA) applied to Western Mediterranean volcanism, concluded that the subduction-related (i.e., orogenic) volcanism shows a greater compositional variability than the intraplate (i.e., anorogenic) volcanism. Compositional variation in orogenic volcanism is associated with the extensive recycling of geochemically different lithologies producing large heterogeneities in the lithospheric mantle

(Melchiorre et al., 2017). The large variability of chemical composition in the Mediterranean region impedes to assign a unique genetic origin to the volcanism and it has been interpreted as the interaction of multiple processes, partly synchronous, as proposed by several authors (e.g., Duggen et al., 2008; Lustrino et al., 2011; Melchiorre et al., 2017).

The lithospheric mantle composition of the Alboran and Algeria offshore segments is related to their back-arc origin and the degree of partial melting expected from the nature and volume of magmatic events. The space opened between the trench and the upper plate during slab roll-back processes is replaced by fertile sublithospheric mantle with DMM composition that will undergo partial melting by adiabatic decompression. The Algerian Basin shows a typical oceanic crust of ~6 km thickness (Booth-Rea et al., 2007), which corresponds to a ~7% of sublithospheric mantle melting and hence to the DMM-7% composition (Klein and Langmuir, 1987; Workman and Hart, 2005). However, in the Valencia Trough and the Alboran Basin, melting was less extensive producing large magmatic intrusions and volcanism and hence a DMM-6% composition is more likely. These subtle differences in the chemical composition of the lithospheric mantle respond to geodynamic criteria allowing fitting the geophysical observables including the measured P_n seismic velocities (see section 5.3).

During subduction, the slab exchanges heat with the hotter ambient sublithospheric mantle and the temperature of the slab increases while the amplitude of the positive seismic velocity anomaly decreases through time. The precise quantification of these transient effects needs additional data regarding the angle and velocity of subduction (e.g., Boonma et al., 2019) and additional parameters that are poorly constrained (e.g., thermal diffusivity, mantle viscosity, volatile content, etc.).

Both the Alboran and Algerian slabs have been modeled as ~80 km thick bodies centered on the highest positive velocity anomaly and converted to temperature anomalies according to their chemical composition and pressure-temperature conditions resulting in $\Delta T \approx -400$ ºC in both cases (Figures 5 and 6). A similar thermo-chemical anomaly, though with imposed ΔT of -320 ºC and CVP composition, was invoked by Jiménez-Munt et al. (2019) to model the influence of the off-section Alboran slab in the westernmost Alboran Basin along an N-S geo-transect crossing the Gibraltar Strait. It is of interest to highlight the consistency of the seismic velocity anomalies depicted by two independent tomography models based on P-wave travel-time (Alboran slab, e.g., Bezada et al., 2013) and S-wave full-waveform inversion (Algerian slab, Fichtner and Villaseñor, 2015), which result in very similar temperature anomalies corresponding to slabs of comparable ages. Further, DMM-3% composition in the Alboran slab is consistent with the paleogeographic reconstructions proposing highly extended segments in western geo-transect as compared to the fully developed oceanic lithosphere in the eastern geo-transect (i.e. DMM-7% composition of the Algerian slab).

6.3 Geodynamic implications

The present-day structure of the crust and lithospheric mantle in the Western Mediterranean is the result of a long-lived tectonic evolution since the stretching and spreading of the Ligurian-Tethys Ocean from Jurassic to present. The analyzed geo-transects mostly show the present-day crust resultant from the protracted Africa-Europe convergence during the Late Cretaceous-Cenozoic period, building the Betics-Rif and Kabylies-Tell-Atlas subduction-related orogenic systems. On the contrary, the current upper mantle structure is mostly post-tectonic, resulting from the lithosphere-asthenosphere interaction governed by the subduction and further rollback of the Ligurian-Tethys lithosphere.

The Alboran Basin has experienced different and partly coeval geodynamic processes including the subduction and further roll-back, continental mantle delamination and slab break-off of the Ligurian-Tethys slab. The high density Internal Betics, mostly characterized by Palaeozoic and pre-Upper Triassic HP/LT metamorphic rocks, are interpreted to represent the highly extended Iberian distal margin that underwent partial subduction and exhumation along the subduction interface (Vergés and Fernàndez, 2012; Figure 8), as evidenced from P-T-t paths and ages of HP/LT metamorphic peaks (summary in Gómez-Pugnaire et al., 2019). The exhumed HP/LT metamorphic units formed a roughly NNW-directed stack of relatively thin tectonic nappes, each nappe recording specific metamorphic histories. The relatively low-density External Units in the Betics is constituted by a thick sedimentary sequence starting in the Upper Triassic evaporites that corresponds to the main detachment level of the Betics at the scale of the whole orogenic system and behaving as an important decoupling layer during subduction (Vergés and Fernàndez, 2012; Ruiz-Constán et al., 2012).

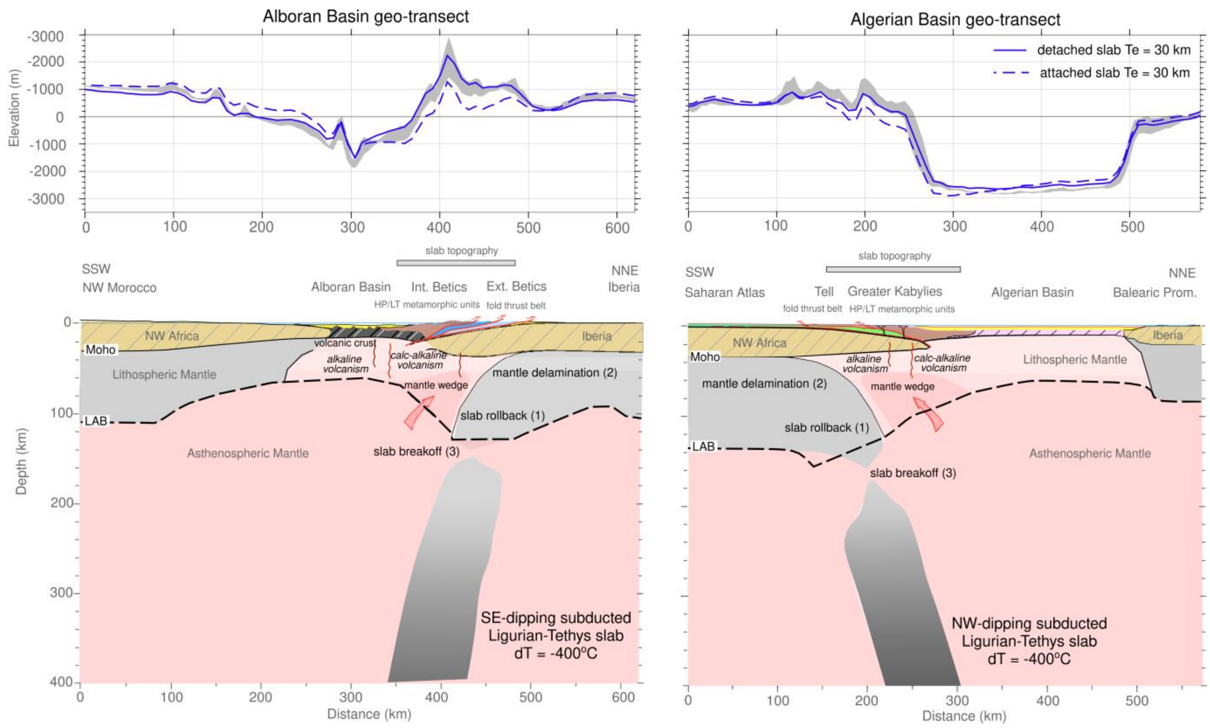

Figure 8. Crustal and lithospheric cross-sections at scale along modeled Algerian Basin-Kabylies-Tell-Atlas and Alboran Basin-Internal Betics-External Betics-foreland geo-transects. The structure of both margins is similar and comparable implying that the underlying geodynamic processes are similar for both margins.

The density contrast between the External Betics and the underlying basement vanishes at mid-crustal levels (15-20 km depth) because of the considered pressure-dependent density (Table 1, Figure S8). Though this reduces the ability of gravity modeling in determining the geometry of the External Betics at depth, underthrusting of the sedimentary cover is conceptually consistent with the NW retreat of the Alboran slab. Indeed, clustering of the seismicity in the External Betics, beneath the Internal Units, points to reactivation of faults developed during accretion of the cover. The Betics orogenic system is therefore formed by a system of thrusts that tectonically emplace the Jurassic Ligurian-Tethys extensional depositional domains that configured the SE Iberian margin on top of each other from the most distal margin (Internal Betics) in the hinterland to the proximal margin (External Betics) in the foreland (e.g., García-Hernández et al., 1990; Vergés and Fernàndez, 2012).

The Algerian Basin evolution is triggered by the NW-dipping subduction of the Ligurian-Tethys oceanic segments existing between the Balearic Promontory and the Algerian domain of the NW Africa margin (Alvarez et al., 1974) and is widely accepted by most models (e.g., Vergés and Sàbat, 1999; Frizon de Lamotte et al., 2011; Roure et al., 2012; van Hinsbergen et al., 2014; Casciello et al., 2015; among others). The Kabylies form the HP/LT Internal Units with a relatively high density (Mahdjoub et al., 1997; Michard et al., 2006; Rossetti et al., 2010; Platt et al., 2013; Caby et al., 2014; Fernandez et al., 2016; Bruguier et al., 2017); the Flysch units represent the detached cover above the Ligurian-Tethys sea floor from Jurassic to Late Miocene (e.g., Guerrera and Martín-Martín, 2014, among others), while the Tell and the Atlas form the External Units corresponding to the Algerian margin of the Ligurian-Tethys Ocean (Roure et al., 2012; Leprêtre et al., 2018). For the modeling purposes, the Flysch and External Units are combined since they represent the sedimentary cover of the Algerian continental margin (Figure 4). Similar to the Betics, the Internal Units of the Greater Kabylies Massif are thrusting on the Flysch units, which are further thrusted over the Tellian External Units. Seismicity beneath the Greater Kabylies is distributed in the African basement and the External and Internal units, although it does not show clear clustering probably due to the lack of local seismic recording stations. Earthquakes below Moho close to the present-day passive margin of Algeria could represent the purposed initiation of a new subduction zone (e.g., Déverchère et al., 2005; Hamai et al., 2018).

A common characteristic in both geo-transects is that the crust is thicker in the regions of exhumed HP/LT metamorphic rocks and thins drastically over a short distance to the oceanic/magmatic crust of the back-arc regions in comparison to the gradual thickening in the opposed margins (Figures 4 and 8). Along the Alboran Basin geo-transect, a ~37 km thick crust beneath the Betics thins drastically to a ~16 km magmatic and volcanism intruded crust of the East Alboran Basin that transitions to the thinned continental crust south of the Alboran Ridge and thickens gradually further to the SSE in the NW African margin (e.g., Booth-Rea et al., 2007; Gómez de la Peña et al., 2020). Along the Algerian Basin geo-transect a relatively thick crust of ~30 km beneath northern Algeria (Greater Kabylies) transitions abruptly to ~10 km thick oceanic crust of the Algerian Basin to the NNW (Figure 9). Similarly, thicker lithospheres beneath the Betics and northern Algeria transitions abruptly to only ~60 km thick and fertile lithosphere (i.e., alike to oceanic lithosphere) of both the Alboran and Algerian back-arc basins (Figure 8).

The lithospheric structure beneath the Algeria and SE Iberia margins, though comparable, are different in width and thickness. The Algerian margin is ~200 km wide the SE Iberia margin is only 80 km wide. The maximum lithospheric thickness is ~150 km below Algeria and ~130 km below SE Iberia, although the regional lithospheric thickness of Africa is thicker than in Iberia (Figure 8). The existence of sub vertical detached Ligurian-Tethys lithospheric slabs under the Algeria and SE Iberia margins is another feature of resemblance although they show opposite apparent dip (Figure 8). The two lithospheric slabs are located some tens of km inland from the current shoreline and beneath the high topography region of both orogenic systems (Betics and Kabylies). In both cases the crust is underlain by a relatively fertile lithospheric mantle with compositions close to oceanic lithosphere, whereas towards the respective foreland regions the composition of the mantle is clearly continental. This configuration indicates that the continental lithospheric mantle delaminated once the subduction front collided with the continental mainland. This promoted the inflow of the fertile sublithospheric mantle (mantle wedge) beneath the Iberian and Algerian crusts underlying the HP/LT metamorphic nappes of the Internal Betics and Greater Kabylies (Figure 8). After cessation of subduction the Algerian slab detached and sunk into the sublithospheric mantle whereas the Alboran slab tore in its eastern end and detachment related to tear progressed westwards until its present position.

The lithospheric scale thickening beneath the Greater Kabylies and extensional back-arc oceanic Algerian Basin is consistent with SE retreating subduction kinematics, hence can be explained by all the three geodynamic scenarios proposed for the Western Mediterranean evolution (Figures 1b and 8). However, each of these models imply different lithospheric structures along the Alboran Basin geo-transect. The geodynamic model with a single long subduction, scenario 2, covering both the Alboran and Algerian basins, retreating to the south cannot explain the NNW vergence of the Internal and External Units of the Betics nor their age of tectonic emplacement, the lithospheric structure, and the position of the Alboran slab beneath the Betics (Figure 1b, scenario 2). Whereas the other two models, scenario 1 and scenario 3, are consistent with the structure beneath the Betics, they imply incompatible lithospheric structures along the NW Africa margin. According to scenario 1 (Figure 1b, van Hinsbergen et al., 2014), the Alboran slab segment retreated to the west along the purposed North Africa transform fault, i.e. Subduction-Transform Edge Propagator, or STEP fault (Govers and Wortel, 2005), before colliding with the Iberian margin. This transform fault or edge propagator should produce a sharp change in the crust and lithospheric mantle structure beneath the African margin, between the Rif and Tell-Atlas Mountains, which is contrary to the observed gradual lithospheric thinning in our lithospheric structure model (Figure 8) (see also Fernàndez et al., 2019 for a more complete discussion).

The opposite direction of slab retreat in the adjacent segments proposed by scenario 3 (Figure 1b, Vergés and Fernàndez, 2012) implies opposite symmetry in the crust and upper mantle structure as observed in our models (Figure 8). Scenario 3 is based on the pre-convergence geometry of the Iberia-Africa Ligurian-Tethys, characterized by a markedly segmented margin configuration (Frizon de Lamotte et al., 2011; Schettino and Turco, 2011; Vergés and Fernàndez, 2012; Fernàndez et al., 2019; Fernandez, 2019; Martín-Chivelet et al., 2019; Ramos et al., 2020; Pedrera et al., 2020). This margin segmentation exerted a strong control on the further evolution of the Ligurian-Tethys realm allowing for opposed subduction polarities in adjacent segments. The dynamics of such subduction system has been studied using analogue and numerical experiments by Peral et al. (2018) and Peral et al. (2020). The observed lithospheric scale thickening beneath the HP/LT metamorphic rocks of the Betics followed by extension driven thinning and abundant volcanism in the Alboran Basin is consistent with the NNW retreat of the Alboran slab. It must be noted that to the west, beneath the Rif mountains, the crust and lithosphere are thick in response to the NW-W retreat of the Alboran slab produced by the higher resistance to slab retreat in the western end of the segment and the consequent trench curvature, which was further tightened by the protracted Iberia–Africa convergence (Kumar et al., 2018; Fernàndez et al., 2019; Peral et al., 2019).

Our results show that because of the break-off of the Algerian slab and the lateral tearing of the Alboran slab most of the vertical stresses related to the slab pull are not transmitted to the overlying lithosphere. The lack of evidence for flexural forebulges in the Alboran and Algerian basins, as inferred by the coupled elevation (Fig. 8 and S4), also hints towards the fact that slabs do not contribute significantly to the flexural isostasy. This mechanical decoupling produces an isostatic rebound that can amount 500–1000 m when considering Te values between 10 km and 30 km or up to 1500–2000 m in the absence of flexural rigidity (Figures 8 and S4). This isostatic rebound can be related to the closure of the Betics corridor and the connection between the Atlantic Ocean and the Mediterranean Sea before the Messinian salinity crisis (García-Castellanos and Villaseñor, 2011). Seismic experiments suggest that the Alboran slab is still attached under the western Betics and the Gibraltar-Rif regions (e.g., Bezada et al., 2013; Palomeras et al., 2014; Mancilla et al., 2015), where average elevation is between 400 m and 800 m lower than in eastern Betics. Similar values of slab pull effects on topography have been proposed for the Western Alboran Basin in relation to the east-dipping Alboran slab along an N-S geo-transect across the Gibraltar Strait (Jiménez-Munt et al., 2019). Estimations from dynamic modeling and residual topography also show values within the estimated range of our work in the study region (e.g., Valera et al., 2011; Civiero et al., 2020; Faccenna and Becker, 2020; Negredo et al., 2020).

7. Conclusions

We presented integrated geophysical-petrological 2D models of the crust and upper mantle structure of the Western Mediterranean along two geo-transects crossing the Alboran and Algerian basins, and the active/orogenic margins of the Betics and Kabylies-Tell-Atlas Mountains, and the passive/conjugate margins of NW Africa and Eastern Iberia (i.e., Balearic Promontory and Valencia Trough), respectively. The new methodology incorporates sublithospheric thermo-chemical anomalies allowing to quantify the impact on geophysical observables of the detached subducting slabs detected from seismic tomography. At the crust level our models differ from previous crustal-scale models highlighting the use of relatively thin Internal Units above sediments of the External Units in the Betics and Greater Kabylies. The resulting models are constrained by geological and geophysical data and are consistent with the surface observables (elevation, gravity, geoid and surface heat flow) and seismic data and tomography models. Different lithospheric mantle compositional domains in accordance with geological domains are required to fit the surface observables. Modeling results show an active interaction between the lithosphere and the underlying sublithospheric mantle which was governed by the Alpine subduction dynamics in addition to the NNW-SSE Africa-Eurasia convergence acting since Late Cretaceous. From the results, the following conclusions have been drawn:

- The thick crust beneath the Betics (~37 km) thins abruptly to16km below the Eastern Alboran Basin, which is modeled as a mostly magmatic crust largely intruded by volcanic rocks, and thickens gradually to ~31 km further to the SSE in NW Morocco. The thick crust beneath the Greater Kabylies (~30 km) is thinning more abruptly to the NNW reaching~10 km below the Algerian Basin, modeled as oceanic crust.
- The lithospheres beneath the Internal Betics and the Greater Kabylies are thick and structures are comparable but showing an opposite symmetry, though the lithospheric thickness is larger below the Greater Kabylies. In SE Iberia, the lithosphere beneath the Betics is ~130 km thick, thinning sharply to the SSE to ~60 km under the Alboran Basin and thickens again, but gradually, towards Africa mainland to ~112 km. Along the Algerian Basin geo-transect, the lithosphere beneath the Greater Kabylies is ~150 km thick and thins to ~60 km thickness to the oceanic lithosphere in the Algerian Basin.
- The present-day lithospheric mantle composition of the Alboran and Algerian basins are modeled as depleted residue from 6-7% aggregate decompressional melting of the more fertile sublithospheric mantle. This is consistent with the back-arc setting of both the Alboran and Algeria basins related to the retreating of the Ligurian-Tethys lithosphere. Slab retreat triggered the melting of the underlying sublithospheric mantle generating

oceanic crust in the Algerian Basin and extensive magmatic and volcanic crust in the Alboran Basin.

- The modeled lithospheric mantle composition beneath the Internal Betics and Greater Kabylies is fertile compared to the corresponding continental lithosphere of the External Betics and Saharan Atlas, respectively. This fertile composition beneath the internal domains of the orogenic systems is consistent with mantle delamination and inland displacement of the slabs during the later stages of subduction and collision, which promoted the inflow of the fertile sublithospheric mantle.
- The detached sub-vertical Ligurian-Tethys lithospheric slabs beneath both orogenic systems (Betics and Kabylies) show, according to tomography models, average temperature and density anomalies of about -400 ºC and +30 kg/m^3 relative to the surrounding mantle. The chemical composition of these slabs is more close to oceanic lithosphere (DMM-3% for the Alboran slab and DMM-7% for the Algerian slab) and therefore more fertile than the subcontinental lithospheric mantle of Iberia and North Africa.
- The Ligurian-Tethys slab beneath the SE Iberia shows an apparent dip to the SSE whereas the slab below Algeria dips to the NNW, matching the tectonic transport direction of the fold and thrust belts of the Betics and Greater Kabylies-Tell-Atlas subduction-related orogens, respectively.
- The large-scale configuration of present-day SE Iberia and Algerian margins as well as their mantle compositions in the Alboran and Algerian geo-transects is consistent with opposite dipping subduction of two segments of the Jurassic Ligurian-Tethys oceanic domain. Their present configurations combined with the tectonic transport directions and shortening estimates on the Betics and Greater Kabylies-Tell-Atlas orogenic systems agree with Neogene slab roll-back processes triggering mantle delamination initiating at the collision stage, followed by slab break-off coinciding with the end of the delamination stage.
- Slab break-off and lateral tearing could be responsible for a minimum uplift of ~700–1000 m in the Betics and ~300-500 m in the Greater Kabylies triggering the closure of the Atlantic-Mediterranean corridor and the Messinian salinity crisis.

8. Credit authorship contribution statement:

Manel Fernàndez and Jaume Vergés designed the study. Ajay Kumar did the modeling using LitMod2D_2.0 (available at https://github.com/ajay6763/LitMod2D_2.0_package_dist_users, https://hub.docker.com/repository/docker/ajay6763/litmod2d_2.0), formal analysis, and wrote the first draft of the manuscript. Jaume Vergés made Figure 8 using commercial Canvas software. Manel Fernàndez, Jaume Vergés, Montserrat Torne and Ivone Jiménez-Munt jointly supervised the work and edited the manuscript.

9. Declaration of competing interest

The authors declare that they have no known competing financial interests or personal relationships that could have appeared to influence the work reported in this paper.

10. Acknowledgements

We acknowledge discussions with Marc Viaplana-Muzas, Jason Williams, Carlos Fernández-García, Kittiphon Boonma, Emilio Casciello, Massimiliano Melchiorre, and Chiara Macchiavelli during the development of this work. This work is funded by the EU Marie Curie Initial Training Network 'SUBITOP' (674899-SUBITOP-H2020-MSCA-ITN-2015) and partly by SUBTETIS (PIE-CSIC-201830E039, CSIC), GeoCAM (PGC2018-095154-B-I00, Spanish Government), Equinor R&T Fornebu (Norway), and the Generalitat de Catalunya grant (AGAUR 2017 SGR 847). This work has been done using the facilities of the Laboratory of Geodynamic Modeling from Geo3BCN-CSIC. Figures were made with the Generic Mapping Tools version 4.0 (www.soest.hawaii.edu/gmt;Wessel and Smith, 1998), Matplotlib (https://matplotlib.org/; Hunter, 2007), and Inkscape (http://www.inkscape.org/; Harrington et al., 2004, 2005).

11. Data Availability

Data used in this work can be found in references cited in the main text and figure captions. Publically available data can be found at https://www.ngdc.noaa.gov/mgg/global/global.html for elevation; http://icgem.gfz-potsdam.de/home for geoid height; and https://www.ihfc-iugg.org/products/global-heat-flow-database for surface heat flow.

12. References

Afonso, J. C., Fernàndez, M., Ranalli, G., Griffin, W. L., & Connolly, J. A. D. (2008). Integrated geophysical-petrological modeling of the lithosphere and sublithospheric upper mantle: Methodology and applications. Geochemistry, Geophysics, Geosystems, 9, Q05008.

Afonso, J. C., Fullea, J., Griffin, W. L., Yang, Y., Jones, A. G., Connolly, J. A. D., & O'Reilly, S. Y. (2013a). 3-D multiobservable probabilistic inversion for the compositional and thermal structure of the lithosphere and upper mantle. I: A priori petrological information and geophysical observables. Journal of Geophysical Research: Solid Earth, 118,2586–2617. https://doi.org/10.1002/ jgrb.50124

Afonso, J. C., Fullea, J., Yang, Y., Connolly, J. A. D., & Jones, A. G. (2013b). 3-D multi-observable probabilistic inversion for the compositional and thermal structure of the lithosphere and upper mantle. II: General methodology and resolution analysis. Journal of Geophysical Research: Solid Earth, 118, 1650–1676.

Afonso, J. C., & Zlotnik, S. (2011). The subductability of the continental lithosphere: The before and after story. In D. Brown & P. D. Ryan (Eds.), Arc-Continent Collision (pp. 53–86). Berlin: Frontiers in Earth Sciences, Springer.

Agard, P., Plunder, A., Angiboust, S., Bonnet, G.,& Ruh, J. (2018). The subduction plate interface: rock record and mechanical coupling (from long to short timescales). Lithos, 320-321, 537-566.

Aïdi, C., Beslier, M. O., Yelles-Chaouche, A. K., Klingelhoefer, F., Bracene, R., Galve, A., Bounif, A., Schenini, L., Hamai, L., Schnurle, P., Djellit, H., Sage, F., Charbis, P., & Déverchère, J., (2018). Deep structure of the continental margin and basin off Greater Kabylia, Algeria–New insights from wide-angle seismic data modeling and multichannel seismic interpretation. Tectonophysics, 728, 1-22.

Alvarez, W., Cocozza, T., & Wezel, F. C. (1974). Fragmentation of the Alpine orogenic belt by microplate dispersal. Nature, 248(5446), 309-314.

Amante, C. & Eakins, B. W., 2009. ETOPO1 1 Arc-minute global relief model: Procedures, data sources and analysis. NOAA Technical Memorandum NESDIS NGDC-24, http://www.ngdc.noaa.gov/mgg/global/global.html

Amaru, M. L. (2007). Global travel time tomography with 3-D reference models (Vol. 274). Utrecht University.

Ayala, C., Bohoyo, F., Maestro, A., Reguera, M. I., Rubio, F. M., Torne, M., et al. (2016). Updated Bouguer anomaly map of the Iberian Peninsula: A new perspective to interpret the regional geology. Journal of Maps. https://doi.org/10.1080/17445647.2015.1126538

Balanyá, J. C., & García-Dueñas, V. (1987). Les directions structurales dans le Domaine d'Alborán de part et d'autre du Détroit de Gibraltar. Comptes rendus de l'Académie des sciences. Série 2, Mécanique, Physique, Chimie, Sciences de l'univers, Sciences de la Terre, 304(15), 929-932.

Banda, E., Gallart, J., Garcia-Duenas, V., Danobeitia, J.J., Makris, J., (1993). Lateral variation of the crust in the Iberian Peninsula. New evidence from the Betic Cordillera. Tectonophysics 221, 53–66

Banks, C.J.,& Warburton, J., 1991. Mid-crustal detachment in the Betic system of southeast Spain. Tectonophysics 191, 275–289.

Berástegui, X., Banks, C.J., Puig, C., Taberner, C., Waltham, D., &Fernandez, M., (1998). Lateral diapiric emplacement of Triassic evaporites at the southern margin of the Guadalqui- vir Basin, Spain. In: Mascle, A., Puigdefabregas, C., Luterbacher, H., Fernandez, M. (Eds.), Cenozoic Foreland Basins of Western Europe. Geological Society Special Publications 134, pp. 49–68.

Bezada, M. J., Humphreys, E. D., Toomey, D. R., Harnafi, M., Dávila, J. M., & Gallart, J. (2013).Evidence for slab rollback in westernmost Mediterranean from improved mantle imaging. Earth and Planetary Science Letters, 368,51–60. https://doi.org/10.1016/j. epsl.2013.02.024

Boonma, K., Kumar, A., García-Castellanos, D., Jiménez-Munt, I., & Fernández, M. (2019). Lithospheric mantle buoyancy: the role of tectonic convergence and mantle composition. Scientific reports, 9(1), 1-8.

Booth-Rea, G., Azañón, J.M., Martínez-Martínez, J.M., Vidal, O., & García-Dueñas, V., (2005). Contrasting structural and P–T evolution of tectonic units in the southeastern Betics: key for understanding the exhumation of the Alboran Domain HP/LT crustal rocks (Western Mediterranean). Tectonics 24. http://dx.doi.org/10.1029/2004TC001640.

Booth-Rea, G., Ranero, C. R., Martínez-Martínez, J. M., & Grevemeyer, I. (2007).Crustal types and Tertiary tectonic evolution of the Alborán sea, western Mediterranean. Geochemistry, Geophysics, Geosystems, 8(10).

Bruguier, O., Bosch, D., Caby, R., Vitale-Brovarone, A., Fernandez, L., Hammor, D., & Mechati, M. (2017). Age of UHP metamorphism in the Western Mediterranean: insight from rutile and minute zircon inclusions in a diamond-bearing garnet megacryst (Edough Massif, NE Algeria). Earth and Planetary Science Letters, 474, 215-225.

Brun, J. P., & Faccenna, C. (2008).Exhumation of high-pressure rocks driven by slab rollback. Earth and Planetary Science Letters, 272(1-2), 1-7.

Caby, R., Bruguier, O., Fernandez, L., Hammor, D., Bosch, D., Mechati, M.,& Douchet, C. (2014). Metamorphic diamonds in a garnet megacryst from the Edough Massif (northeastern Algeria). Recognition and geodynamic consequences. Tectonophysics, 637, 341-353.

Calvert, A., Sandvol, E., Seber, D., Barazangi, M., Roecker, S., Mourabit, T., Vidal, F., Alguacil, G.,&Jabour, N., (2000). Propagation of regional seismic phases (Lg and Sn) and Pn velocity structure along the Africa–Iberia plate boundary zone. Geophysical Journal International 142, 384–408.

Casciello, E.; Fernàndez, M.; Vergés, J.; Cessarano, M.; &Torne, M. (2015). The Alboran Domain in the Western Mediterranean evolution: The birth of a concept. Bull. Soc. Géol., 186, 23–34.

Carballo, A., Fernandez, M., Torne, M., Jiménez-Munt, I., & Villaseñor, A. (2015a). Thermal and petrophysical characterization of the lithospheric mantle along the northeastern Iberia geo-transect. Gondwana Research, 27, 1430-1445.

Carballo, A., Fernandez, M., Jiménez-Munt, I., Torne, M., Vergés, J., Melchiorre, M., et al. (2015b). From the North-Iberian Margin to the Alboran Basin: A lithosphere geo-transect across the Iberian Plate. Tectonophysics, 399-418.

Carbonell, R., Torne, M., García-Dueñas, V., Moya, R., Banda, E., (1997). The ESCI-Béticas: a seismic reflection image of the Betics orogen. Rev. Soc. Geol. Esp. 8, 503–512.

Carbonell, R., Sallarès, V., Pous, J., Dan, J. J., Queralt, P., Ledo, J. J., & Duen, V. G. (1998). A multidisciplinary geophysical study in the Betic chain (southern Iberia Peninsula). Tectonophysics, 288(1-4), 137-152.

Chazot, G., Abbassene, F., Maury, R. C., Déverchère, J., Bellon, H., Ouabadi, A., & Bosch, D. (2017). An overview on the origin of post-collisional Miocene magmatism in the Kabylies (northern Algeria): evidence for crustal stacking, delamination and slab detachment. Journal of African Earth Sciences, 125, 27-41.

Chertova, M.V., Spakman, W., Geenen, T., van den Berg, A.P., &van Hinsbergen, D.J.J. (2014). Underpinning tectonic reconstructions of the western Mediterranean region with dynamic slab evolution from 3-D numerical modeling. J. Geophys. Res.: Solid Earth, 119, 5876–5902.

Civiero, C., Strak, V., Custódio, S., Silveira, G., Rawlinson, N., Arroucau, P., & Corela, C. (2018). A common deep source for upper-mantle upwellings below the Ibero-western Maghreb region from teleseismic P-wave travel-time tomography. Earth and Planetary Science Letters, 499, 157-172.

Civiero, C., Custódio, S., Duarte, J. C., Mendes, V. B., & Faccenna, C. (2020). Dynamics of the Gibraltar Arc System: A Complex Interaction Between Plate Convergence, Slab Pull, and Mantle Flow. Journal of Geophysical Research: Solid Earth, 125(7), e2019JB018873.

Comas, M.C., Dañobeitia, J.J., Alvarez-Marrón, J., &Soto, J.I., (1995). Crustal reflections and structure in the Alboran Basin: Preliminary Results of the SCI-Alboran Survey. In: Santanach, P. (Ed.). Revista de la Sociedad Geológica de España 8, pp. 75–88

Connolly, J. A. D. (2005). Computation of phase equilibria by linear programming: A tool for geodynamic modeling and its application to subduction zone decarbonation. Earth and Planetary Science Letters, 236 (1-2), 524-541.

Connolly, J. A. D. (2009). The geodynamic equation of state: What and how, Geochem. Geophys.Geosyst., 10, Q10014,doi:10.1029/2009GC002540.

Coulon, C., Megartsi, M., Fourcade, S., Maury, R.C., Bellon, H., Louni-Hacini, A., Cotten, J., Coutelle,A., &Hermitte,D., (2002). Post-collisional transition from calc-alkaline to alkaline volcanism during the Neogene in Oranie (Algeria): magmatic expression of a slab breakoff. Lithos 62, 87–110.

Dañobeitia, J.J., Arguedas, M., Gallart, F., Banda, E., &Makris, J., (1992).Deep crustal configuration of the Valencia trough and its Iberian and Balearic borders from extensive refraction and wide-angle reflection profiling. Tectonophysics 203, 37–55.

Déverchère, J., Yelles, K., Domzig, A., Mercier de Lépinay, B., Bouillin, J.P., Gaullier, V., Bracène, R., Calais, E., Savoye, B., Kherroubi, A. & Le Roy, P., 2005. Active thrust faulting offshore Boumerdes, Algeria, and its relations to the 2003 Mw 6.9 earthquake. Geophysical research letters, 32(4).

Diaz, J., Gallart, J., & Carbonell, R. (2016). Moho topography beneath the Iberian-Western Mediterranean region mapped from controlled- source and natural seismicity surveys. Tectonophysics, 692,74–85. https://doi.org/10.1016/j.tecto.2016.08.023

Díaz, J., &Gallart, J. (2009). Crustal structure beneath the Iberian Peninsula and surrounding waters: a new compilation of deep seismic sounding results. Phys. Earth Planet. Sci. Lett.173,181–190. http://dx.doi.org/10.1016/j.pepi. 2008.11.008.

Díaz, J., Gil, A., &Gallart, J. (2013).Uppermost mantle seismic velocity and anisotropy in the Euro-Mediterranean region from Pn and Sn tomography. Geophys. J. Int. http://dx. doi.org/10.1093/gji/ggs016.

Duggen, S., Hoernle, K., van den Bogaard, P., & Garbe-Schönberg, D. (2005). Post-collisional transition from subduction- to intraplate-type magmatism in the westernmost Mediterranean: Evidence for continental-edge delamination of subcontinental lithosphere. Journal of Petrology, 46, 1155–1201. https://doi.org/10.1093/petrology/egi013

Duggen, S., Hoernle, K. A., Klugel, A., Geldmacher, J., Thirlwall, M. F., Hauff, F., et al. (2008). Geochemical zonation of the Miocene Alborán Basin volcanism (westernmost Mediterranean): Geodynamic implications. Contributions to Mineralogy and Petrology, 156, 577–593. https://doi.org/10.1007/s00410-008-0302-4

Eaton, D. W., Darbyshire, F., Evans, R. L., Grütter, H., Jones, A., & Yuan, X. (2009).The elusive lithosphere-asthenosphere boundary (LAB) beneath cratons.Lithos, 109,1–22.https://doi.org/10.1016/j.lithos.2008.05.009

Ehsan, S. A., Carbonell, R., Ayarza, P., Martí, D., Jesús Martínez-Poyatos, D., Simancas, J., et al. (2015). Lithospheric velocity model across the Southern Central Iberian Zone (Variscan Iberian Massif): The ALCUDIA wide-angle seismic reflection transect. Tectonics, 34, 535–554. https://doi.org/10.1002/2014TC003661

Etheve, N., Mohn, G., Frizon de Lamotte, D., Roca, E., Tugend, J., & Gómez-Romeu, J. (2018). Extreme Mesozoic crustal thinning in the eastern Iberia margin: the example of the Columbrets Basin (Valencia Trough). Tectonics, 37(2), 636-662.

Faccenna, C., & Becker, T. W. (2020). Topographic expressions of mantle dynamics in the Mediterranean. Earth-Science Reviews, 103327.

Faccenna, C., Piromallo, C., Crespo-Blanc, A., Jolivet, L., & Rossetti, F. (2004). Lateral slab deformation and the origin of the western Mediterranean arcs. Tectonics, 23(1).

Fernandez, L., Bosch, D., Bruguier, O, Hammor, D., Caby, R., Monié, P., et al. (2016). Permo-carboniferous and early miocene geological evolution of the internal zones of the Maghrebides-new insights on the western Mediterranean evolution. Journal of Geodynamics 96: 146–173.

Fernández-García, C., Guillaume, B., & Brun, J. P. (2019).3D slab breakoff in laboratory experiments. Tectonophysics, 773, 228223.

Fernàndez, M., Berástegui, X., Puig, C., García-Castellanos, D., Jurado, M.J., Torné, M., &Banks, C., (1998a). Geophysical and geological constraints on the evolution of the Guadalquivir foreland basin, Spain. In: Mascle, A., Puigdefàbregas, C., Luterbacher, H.P., Fernàndez, M. (Eds.), Cenozoic Foreland Basins ofWestern Europe: Geological Society Special Publications, 134, pp. 29–48.

Fernàndez, M., Marzan, I., Correia, A., &Ramalho, E., (1998b). Heat flow, heat production, and lithospheric thermal regime in the Iberian Peninsula.Tectonophysics 291, 29–53. http://dx.doi.org/10.1016/S0040-1951(98)00029-8.

Fernàndez, M., & Cabal, J. (1992).Heat-flow data and shallow thermal regime on Mallorca and Menorca (western Mediterranean). Tectonophysics, 203(1-4), 133-143.

Fernàndez, M., Foucher, J.P. & Jurado, M.J. (1995).Evidence for the multi-stage formation of the south- western Valencia Trough.Marine and Petroleum Geology, 12,101-109.

Fernàndez, M., Torne, M., Vergés, J., Casciello, E., & Macchiavelli, C. (2019).Evidence of Segmentation in the Iberia–Africa Plate Boundary: A Jurassic Heritage? Geosciences, 9(8), 343.

Fichtner, A., &Villaseñor, A., (2015). Crust and upper mantle of the western Mediterranean - constraints from full-waveform inversion. Earth Planet.Sci. Lett. 428, 52–62.

Foucher, J.E., Mauffret, A., Steckler, M., Brunet, M.E., Maillard, A., Rehanlt, J.E., Alonso, B., Desegaulx, E., Murillas, J., &Ouillon, G., (1992). Heat flow in the Valencia trough: geodynamic implications. Tectonophysics 203, 77–97.

Fourcade, S., Capdevila, R., Ouabadi, A., & Martineau, F. (2001).The origin and geodynamic significance of the Alpine cordierite-bearing granitoids of northern Algeria.A combined petrological, mineralogical, geochemical and isotopic (O, H, Sr, Nd) study. Lithos, 57(2-3), 187-216.

Frizon de Lamotte, D., Crespo-Blanc, A., Saint-Bezar, B., Comas, M., Fernandez, M., Zeyen, H., Ayarza, P., Robert-Charrue, C., Chalouan, A., Zizi, M., Teixell, A., Arboleya, M.L., Alvarez-Lobato, F., Julivert, M., & Michard, A., (2004).TRASNSMED-transect I (Betics, Alboran Sea, Rif, Moroccan Meseta, High Atlas, Jbel Saghro, Tindouf basin). In: Cavazza, W., Roure, F., Spakman, W., Stampfli, G.M., Ziegler, P.M. (Eds.), The TRANSMED Atlas- the Mediterranean region from Crust to Mantle. Springer, Berlin Heildelberg.

Frizon de Lamotte, D., Raulin, C., Mouchot, N., Wrobel-Daveau, J.-C., Blanpied, C., Ringenbach, J.C., (2011). The southernmost margin of the Tethys realm during the Mesozoic and Cenozoic: initial geometry and timing of the inversion processes. Tectonics 30, TC3002. http://dx.doi.org/10.1029/2010TC002691.

Fullea, J., Fernàndez, M., Afonso, J. C., Vergés, J., & Zeyen, H. (2010). The structure and evolution of the lithosphere–asthenosphere boundary beneath the Atlantic–Mediterranean Transition Region. Lithos, 120(1-2), 74-95.

Fullea, J., Fernàndez, M., & Zeyen, H. (2008). FA2BOUG—A FORTRAN 90 code to compute Bouguer gravity anomalies from gridded free air anomalies: Application to the Atlantic–Mediterranean transition zone. Computers & Geosciences, 34, 1665–1681. https://doi.org/ 10.1016/j.cageo.2008.02.018

Fullea, J., Fernandez, M., Zeyen, H., & Vergés, J. (2007). A rapid method to map the crustal and lithospheric thickness using elevation, geoid anomaly and thermal analysis.Application to the Gibraltar Arc System, Atlas Mountains and adjacent zones. Tectonophysics, 430(1-4), 97-117.

Gallart, J., Vidal, N., Dañobeitia, J.J., (1995). Multichannel seismic imageof the crustal thin- ning at the NE Iberian margin combining normal and wide angle reflection data.Geophys. Res. Lett. 22, 489–492.

Garcia-Castellanos, D., Fernandez, M., & Torne, M. (2002). Modeling the evolution of the Guadalquivir foreland basin (southern Spain).Tectonics, 21 (3).

Garcia-Castellanos, D., & Villasenor, A. (2011). Messinian salinity crisis regulated by competing tectonics and erosion at the Gibraltar arc., Nature, 480(7377), 359–363. https://doi.org/10.1038/nature10651

García-Hernández, M., López-Garrido, A. C., Rivas, P., Sanz de Galdeano, C., & Vera, J. A. (1980). Mesozoic palaeogeographic evolution of the External Zones of the Betic Cordillera. Geology En Mijnbouw, 59(2), 155–168.

Gaspar-Escribano, J. M., Garcia-Castellanos, D., Roca, E., & Cloetingh, S. A. P. L. (2004). Cenozoic vertical motions of the Catalan Coastal Ranges (NE Spain): The role of tectonics, isostasy, and surface transport. Tectonics, 23(1).

Gilardoni, M., Reguzzoni, M., & Sampietro, D. (2016). GECO: A global gravity model by locally combining GOCE data and EGM2008. Studia Geophysica et Geodaetica, 60, 228–247. https://doi.org/10.1007/s11200-015-1114-4

Globig, J., Fernàndez, M., Torne, M., Vergés, J., Robert, A., & Faccenna, C. (2016). New insights into the crust and lithospheric mantle structure of Africa from elevation, geoid, and thermal analysis. Journal of Geophysical Research-Solid Earth, 121, 5389–5424. https://doi. org/10.1002/2016JB012972

Gómez de la Peña, L., Ranero, C. R., & Gràcia, E. (2018).The crustal domains of the Alboran Basin (western Mediterranean). Tectonics, 37, 3352–3377. https://doi.org/10.1029/2017TC004946

Govers, R., Wortel, M., 2005. Lithosphere tearing at STEP faults: response to edges of subduction zones. Earth Planet. Sci. Lett. 236, 505–523. doi:10.1016/j.epsl.2005.03.022

Gueguen, E., Doglioni, C., Fernandez, M., (1998). On the post-25 Ma geodynamic evolution of the western Mediterranean. Tectonophysics 298, 259–269.

Guerrera, F., & Martín-Martín, M. (2014). Geodynamic events reconstructed in the Betic, Maghrebian, and Apennine chains (central-western Tethys). Bulletin de la Société géologique de France, 185(5), 329-341.

Griffin, W., O'Reilly, S., Afonso, J., & Begg, G. (2009). The composition and evolution of lithospheric mantle: A re-evaluation and its tectonic implications. Journal of Petrology, 50 (7), 1185-1204.

Hamai, L., Petit, C., Le Pourhiet, L., Yelles-Chaouche, A., Déverchère, J., Beslier, M. O., & Abtout, A. (2018). Towards subduction inception along the inverted North African margin of Algeria?Insights from thermo-mechanical models. Earth and Planetary Science Letters, 501, 13-23.

Hatzfeld, D., & the Working Group for Deep Seismic Sounding, (1978).Crustal seismic profiles in the Alboran Sea — preliminary results. Pure and Applied Geophysics 116, 167–180.

Hinz, K., (1972). Results of seismic refraction investigations (Project Anna) in Western Mediterranean, south and north of the island of Mallorca.Bulletin Centre De Recherches Pau-SNPA 6 (2), 405–426.

Holland, T., & Powell, R. (1998). An internally consistent thermodynamic data set for phases of petrological interest. Journal of Metamorphic Geology, 16 (3), 309-343.

Ince, E. S., Barthelmes, F., Reißland, S., Elger, K., Förste, C., Flechtner, F., & Schuh, H. (2019). ICGEM—15 years of successful collection and distribution of global gravitational models, associated services and future plans. Earth System Science Data, 11, 647–674. http://doi. org/10.5194/essd-11-647-2019

Jackson, I., & Faul, U. (2010). Grainsize-sensitive viscoelastic relaxation in olivine: Towards a robust laboratory-based model for seismological application. Physics of the Earth and Planetary Interiors, 183, 151-163.

Jolivet, L., C. Faccenna, & C. Piromallo (2009), From mantle to crust: Stretching the Mediterranean, Earth Planet. Sci. Lett., 285, 198–209, doi:10.1016/j.epsl.2009.06.017.

Jolivet, L., & Faccenna, C., (2000). Mediterranean extension and the Africa-Eurasia collision.Tectonics 19, 1094e1106.

Jiménez-Munt,I.,M. Fernàndez, J. Vergés, J. C. Afonso, D. Garcia-Castellanos, andJ. Fullea (2010), Lithospheric structure of the Gorringe Bank:Insights into its origin and tectonic evolution, Tectonics, 29,TC5019, doi:10.1029/2009TC002458

Jiménez-Munt, I., Torne, M., Fernàndez, M., Vergés, J., Kumar, A., Carballo, A., &García-Castellanos, D., (2019). Deep Seated Density Anomalies Across the Iberia-Africa Plate Boundary and Its Topographic Response. J. Geophys. Res. Solid Earth 124, 13310–13332. doi:10.1029/2019JB018445

Kaban, M. K., Chen, B., Tesauro, M., Petrunin, A. G., El Khrepy, S., & Al-Arifi, N.(2018). Reconsidering effective elasticthickness estimates by incorporatingthe effect of sediments: A case study forEurope. Geophysical Research Letters, 45,9523–9532,doi:10.1029/2018GL079732

Khomsi, S., Roure, F., Khelil, M., Mezni, R., & Echihi, O., 2019. A review of the crustal architecture and related pre-salt oil/gas objectives of the eastern Maghreb Atlas and Tell: Need for deep seismic reflection profiling. Tectonophysics 766, 232–248. doi:10.1016/j.tecto.2019.06.009

Klein, E., & Langmuir, C. (1987). Global correlations of ocean ridge basalt chemistry with axial depth: A new perspective. Journal of Geophysical Research, 92(B8), 8089–8115.

Kumar, A.; Fernandez, M.; Peral, M.; Funiciello, F.; Zlotnik, S.; Faccenna, C.; Vergés, J. (2018). Effects of kinematic boundary conditions on trench curvature in a retreating subduction zone: insights from analog modelling. American Geophysical Union, Fall Meeting 2018, abstract #DI51B-0012, 2018AGUFMDI51B0012K.

Kumar, A., Fernàndez, M., Jimenez-Munt, I., Torne, M., Vergés, J., & Afonso, J. C. (2020). LitMod2D_2. 0: An improved integrated geophysical-petrological modeling tool for the physical interpretation of upper mantle anomalies. Geochemistry, Geophysics, Geosystems, e2019GC008777, doi: 10.1029/2019GC008777

Laouar, R., Boyce, A.J., Arafa, M., Ouabadi, A., &Fallick, A.E., (2005).Petrological, geochemical, stable isotope constraints on the genesis of the Miocene igneous rocks ofChetaibi and Cap de Fer (NE Algeria). J. Afr. Earth Sci. 41, 445–465.

Le Roux, V., Bodinier, J.-L., Tommasi, A., Alard, O., Dautria, J.-M., Vauchez, A., &Riches, A.J.V., (2007). The Lherz spinel lherzolite: refertilised rather than pristine mantle. Earth and Planetary Science Letters 259, 599–612.

Leprêtre, R., de Lamotte, D. F., Combier, V., Gimeno-Vives, O., Mohn, G., & Eschard, R. (2018). The Tell-Rif orogenic system (Morocco, Algeria, Tunisia) and the structural heritage of the southern Tethys margin.

Lustrino, M., Duggen, S., & Rosenberg, C. L. (2011). The Central-Western Mediterranean: anomalous igneous activity in an anomalous collisional tectonic setting. Earth-Science Reviews, 104(1-3), 1-40.

Lustrino, M., & Wilson, M. (2007).The circum-Mediterranean anorogenic Cenozoic igneous province. Earth-Science Reviews, 81(1-2), 1-65.

Macchiavelli, C., Vergés, J., Schettino, A., Fernàndez, M., Turco, E., Casciello, E., Tone, M., Pietrantoni, P.P., & Tunini, L. (2017). A new southern North Atlantic isochron map: Insights into the drift of the Iberian plate since the Late Cretaceous. Journal of Geophysical Research: Solid Earth, 122(12), 9603-9626.

Magni, V. (2019).The effects of back-arc spreading on arc magmatism. Earth and Planetary Science Letters, 519, 141-151.

Mahdjoub, Y., Choukroune, P., & Kienast, J. R. (1997).Kinematics of a complex Alpine segment; superimposed tectonic and metamorphic events in the Petite Kabylie Massif (northern Algeria). Bulletin de la Société Géologique de France, 168(5), 649-661.

Mancilla, F.d.L., Booth-Rea, G., Stich, D., Pérez-Peña, J. V., Morales, J., Azañón, J. M., Martin, R., & Giaconia, F. (2015). Slab rupture and delamination under the Betics and Rif constrained from receiver functions. Tectonophysics, 663, 225-237.

Mancilla, F. d. L., Heit, B., Morales, J., Yuan, X., Stich, D., Molina-Aguilera, A., Azañon, J. M., & Martín, R. (2018). A STEP fault in Central Betics, associated with lateral lithospheric tearing at the northern edge of the Gibraltar arc subduction system. Earth and Planetary Science Letters, 486, 32-40.

Martí, J., Mitjavila, J., Roca, E. and Aparicio, C., (1992). Cenozoic magmatism of the Valencia trough (western Mediterranean): relationship between structural evolu- tion and volcanism. Tectonophysics, 203, 145-165.

Martínez-García, P., Comas, M., Lonergan, L., & Watts, A. B. (2017). From Extension to Shortening: Tectonic Inversion Distributed in Time and Space in the Alboran Sea, Western Mediterranean. Tectonics, 36(12), 2777–2805. https://doi.org/10.1002/2017TC004489

Maury, R.C., Fourcade, S., Coulon, C., El Azzouzi, M., Bellon, H., Coutelle, A., Ouabadi, A., Semroud, B., Megartsi, M., Cotton, J., Belanteur, O., Louni-Hacini, A., Piqué, A., Capdevila, R., Hernandez, J., &Réhault, J.P., (2000). Post-collisional Neogene mag- matism of the Mediterranean Maghreb margin: a consequence of slab breakoff.CR Acad. Sci. Paris 331, 159–173.

Marzán, I., (2000). Régimen térmico en la Península Ibérica. Estructura litosférica a través del Macizo Ibérico y el Margen Sur-portugués. Tesis Doctoral Universidad de Barcelona (192 pp.).

McDonough, W., & Sun, S., (1995). The composition of the Earth'. Chemical Geology 120 (120), 223-253.

Michard, A., Negro, F., Saddiqi, O., Bouybaouene, M. L., Chalouan, A., Montigny, R., & Goffé, B. (2006). Pressure–temperature–time constraints on the Maghrebide mountain building: evidence from the Rif–Betic transect (Morocco, Spain), Algerian correlations, and geodynamic implications. Comptes Rendus Geoscience, 338(1-2), 92-114.

Michard, A.,Chalouan, A.,Feinberg, H.,Goffé,B., &Montingny, R., (2002). How does the Alpine belt end between Spain and Morocco.Bulletin de la Société Géologique de France 173, 3–15.

Melchiorre, M., Vergés, J., Fernàndez, M., Coltorti, M., Torne, M., & Casciello, E. (2017).Evidence for mantle heterogeneities in the wes- ternmost Mediterranean from a statistical approach to volcanic petrology.Lithos, 276,62–74. https://doi.org/10.1016/j.lithos.2016.11.018

Moudnib, L. E., Villaseñor, A., Harnafi, M., Gallart, J., Pazos, A., Serrano, I.,Córdoba, D., Pulgar, J. A., Ibarra, P., Himmi, M. N., & Chourak, M. (2015). Crustal structure of the Betic–Rif system, western Mediterranean, from local earthquake tomography. Tectonophysics, 643, 94-105.

Negredo, A. M., Mancilla, F. D. L., Clemente, C., Morales, J., & Fullea, J. (2020).Geodynamic modelling of edge-delamination driven by STEP faults: the westernmost Mediterranean margin (central Betic orogen) case study. Frontiers in Earth Science, 8, 435.

Niu, Y. (1997). Mantle melting and melt extraction processes beneath ocean ridges: Evidence from abyssal peridotites. Journal of Petrology, 38 (8), 1047-1074.

Palomeras, I., Villaseñor, A., Thurner, S., Levander, A., Gallart, J., & Harnafi, M. (2017). Lithospheric structure ofIberia and Morocco using finite-frequency Rayleigh wave tomography from earthquakes and seismic ambient noise. Geochemistry, Geophysics, Geosystems, 18, 1824–1840. https://doi.org/10.1002/2016GC006657

Palomeras, I., Thurner, S., Levander, A., Liu, K., Villaseñor, A., Carbonell, R., & Harnafi, M. (2014). Finite-frequency Rayleigh wave tomography of the western Mediterranean: Mapping its lithospheric structure. Geochemistry, Geophysics, Geosystems, 15(1), 140-160.

Pascal, G., Torne, M., Buhl, P., Watts, A.B. & Mauffret, A. (1992). Crustal and velocity structure of the Valencia Trough (Western Mediterranean). Part II: Detailed interpretation of 5 Expanding Spread Profiles. Tectonophysics. 203, 21-36, DOI: 10.1016/0040-1951(92)90213-P, 1992. Q1; FI: 3.325 - 2.866.

Pascal, G.P., Mauffret, A., &Patriat, P., (1993). The ocean-continent boundary in the Gulf of Lion from analysis of expanding spread profiles and gravity modelling. Geophys. J. Int. 113 (3), 701–726.

Pedrera, A., Ruiz-Constán, A., García-Senz, J., Azor, A., Marín-Lechado, C., Ayala, C., Díaz de Neira, J. A., & Rodríguez-Fernández, L. R. (2020). Evolution of the South-Iberian paleomargin: From hyperextension to continental subduction. Journal of Structural Geology, 13, 104122. https://doi.org/10.1016/j.jsg.2020.104122

Peral, M., Király, Á., Zlotnik, S., Funiciello, F., Fernàndez,M., Faccenna, C., & Vergés, J. (2018). Opposite subduction polarity in adjacent plate segments.Tectonics, 37.https://doi.org/10.1029/ 2017TC004896.

Peral, M., Zlotnik, S., Fernàndez, M., Vergés, J., Kumar, A.,&Ruh, J. (2019).A numerical model of the Western Mediterranean.Geophys. Res. Abstr. 2019, 21, EGU2019-9312.

Peral, M., Ruh, J., Zlotnik, S., Funiciello, F., Fernàndez, M., Vergés, J., & Gerya, T. (2020). Analog and numerical experiments of double subduction systems with opposite polarity in adjacent segments. Geochemistry, Geophysics, Geosystems, e2020GC009035.

Pérez-Gussinyé, M., M. Metois, M. Fernàndez, J. Vergés, J. Fullea, & A. R. Lowry (2009), Effective elastic thickness of Africa and its relationship to other proxies for lithospheric structure and surface tectonics, Earth Planet. Sci. Lett., 287(1-2), 152-167. doi:10.1016/j.epsl.2009.08.004

Piromallo, C., & Morelli, A. (2003).P wave tomography of the mantle under the Alpine-Mediterranean area. Journal of Geophysical Research: Solid Earth, 108(B2).

Platt, J. P., Behr, W. M., Johanesen, K., & Williams, J. R. (2013). The Betic-Rif arc and its orogenic hinterland: a review. Annual Review of Earth and Planetary Sciences, 41, 313-357.

Platt, J.P., Whitehouse, M.J., Kelley, S.P., Carter, A., &Hollick, L., (2003b). Simultaneous extensional exhumation across the Alboran Basin: implications for the causes of late orogenic extension. Geology 31, 251–254.

Poort, J., Lucazeau, F., Le Gal, V., Dal Cin, M., Leroux, E., Bouzid, A., & Ferrante, G. M. (2020). Heat flow in the Western Mediterranean: Thermal anomalies on the margins, the seafloor and the transfer zones. Marine Geology, 419, 106064.

Priestley, K., & McKenzie, D. (2006).The thermal structure of the lithosphere from shear wave velocities. Earth and Planetary Science Letters, 244(1-2), 285–301.

Rimi, A., Fernandez, M., Manar, A., Matsushima, J., Okubo, Y., &Morel, J.L., (2005). Geothermal anomalies and analysis of gravity, fracturing and magnetic features in Morocco. World Geothermal Congress Antalya, Turkey, vol. 2, pp. 4–290.

Ringwood, A. E. (1974). The petrological evolution of island arc systems: Twenty-seventh William Smith Lecture. Journal of the Geological Society, 130(3), 183-204.

Royden, L., & Faccenna, C. (2018). Subduction orogeny and the late cenozoic evolution of the Mediterranean Arcs. Annual Review of Earth and Planetary Sciences, 46, 261-289.

Roca, E. (2001). The Northwest-Mediterranean basin (Valencia Trough, Gulf of Lions and Liguro-Provençal basins): structure and geodynamic evolution. In: Ziegler, P.A., Cavazza, W., Robertson, A.F.H. and Crasquin- Soleau, S. (eds.), Peri Tethyan Rift/Wrench Basins and Passive margins. Mémoires du Muséum National d'Histoire Naturelle, 186, 671-706

Roca, E. (1996). La evolución geodinámica de la Cuenca Catalano-Balear y áreas adyacentes desde el Mesozoico hasta la actualidad. Acta Geológica Hispánica, 29,3-25

Roca, E., Frizon de Lamotte, D., Mauffret, A., Bracène, R., Vergés, J., Benaouali, N., Fernandez, M., Muñoz, J.A., &Zeyen, H., (2004). TRANSMED transect II. In: Cavazza, W., Roure, F., Spakman, W., Stampfli, G.M., Ziegler, P. (Eds.), The TRANSMED Atlas—the Mediterranean Region from Crust to Mantle. Springer, Berlin Heidelberg.

Rossetti, F., Theye, T., Lucci, F., Bouybaouene, M. L., Dini, A., Gerdes, A., ...& Cozzupoli, D. (2010). Timing and modes of granite magmatism in the core of the Alboran Domain, Rif chain, northern Morocco: implications for the Alpine evolution of the western Mediterranean. Tectonics, 29(2).

Roure, F., Casero, P., & Addoum, B. (2012).Alpine inversion of the North African margin and delamination of its continental lithosphere. Tectonics, 31(3).

Ruiz-Constan, A., Pedrera, A., Galindo-Zaldívar, J., Pous, J., Arzate, J., Roldán-García, F.J., Marín-Lechado, C., &Anahnah, F., (2012). Constraints on the frontal crustal structure of a continental collision from an integrated geophysical research: the central-western Betic Cordillera (SW Spain). Geochem.Geophys.Geosyst.13 (8) (art. no. Q08012).

Sàbat, F., Roca, E., Muñoz, J. A., Vergés, J., Santanach, P., & Sans, M. (1995). Margin of Iberia: the ESCI-València Trough seismic profile. Rev. Soc. Geol. España, 8, 4. (not cited)

Sàbat, F., Roca, E., Muñoz, J.A., Vergés, J., Santanach, P., Masana, E., Sans, M., Estévez, A., &Santisteban, C., (1997). Role of extension and compression in the evolution of the east- ern margin of Iberia: the ESCI-València trough seismic profile. Revista de la Sociedad Geológica de España 8, 431–448.

Sandwell, D. T., & Smith, W. H. F. (1997). Marine gravity from Geosat and ERS 1 satellite altimetry.Journal ofGeophysical Research, 102, 10,039–10,054. https://doi.org/10.1029/96jb03223

Schettino, A., &Turco, E.,(2011). Tectonic history of the western Tethys since the Late Triassic. Geol. Soc. Am. Bull., 123, 89–105.

Soto, J.I., &Platt, J.P., (1999) Petrological and structural evolution ofhigh-grade metamorphic rocks from the floor of the Alboran Sea basin, western Mediterranean.Journal of Petrology 40, 21–60.

Spakman, W., & Wortel, M. J. R. (2004).A tomographic view on western Mediterranean geodynamics. In W. Cavazza, F. Roure, W. Spakman, G. M. Stampfli, & P. Ziegler (Eds.), The TRANSMED Atlas—The Mediterranean region from crust to mantle, (pp. 31–52). Berlin Heidelberg: Springer.

Stampfli, G., &Borel, G.D. (2002). A plate tectonic model for the Paleozoic and Mesozoic constrained by dynamic plate boundaries and restored synthetic oceanic isochrones. Earth Planet. Sci. Lett., 196, 17–33.

Spandler, C., & Pirard, C. (2013). Element recycling from subducting slabs to arc crust: A review. Lithos, 170, 208-223.

Teixell, A., Ayarza, P., Zeyen, H., Fernandez, M., & Arboleya, M. L. (2005). Effects of mantle upwelling in a compressional setting: The Atlas Mountains of Morocco. Terra Nova, 17(5), 456-461.

Torne, M., Pascal, G., Buhl, P., Watts, A.B., & Mauffret, A., (1992).Crustal structure of the Valencia Trough (Western Mediterranean).Part 1. A combined refraction/wide angle reflection and near-vertical reflection study. Tectonophysics 203, 1–20.

Torne, M., Banda, E., & Fernandez, M. (1996). The Valencia Trough: geological and geophysical constraints on basin formation models. Mémoires du Muséum national d'histoire naturelle (1993), 170, 103-128.

Torne, M., Fernàndez, M., Vergés, J., Ayala, C., Salas, M. C., Jimenez-Munt, I.,Buffett G.G., & Díaz, J. (2015). Crust and mantle lithospheric structure of the Iberian Peninsula deduced from potential field modeling and thermal analysis. Tectonophysics, 663, 419-433.

Torne, M., Fernàndez, M., Comas, M. C., & Soto, J. I. (2000). Lithospheric structure beneath the Alboran Basin: results from 3D gravity modeling and tectonic relevance. Journal of Geophysical Research: Solid Earth, 105(B2), 3209-3228.

Valera, J. L., Negredo, A. M., & Jiménez-Munt, I. (2011). Deep and near-surface consequences of root removal by asymmetric continental delamination. *Tectonophysics*, *502*(1-2), 257-265.

Van Hinsbergen, D., Vissers, R.,&Spakman, W. (2014).Origin and consequences of western Mediterranean subduction, rollback, and slab segmentation.Tectonics, 33, 393–419.

Vergés, J., Kullberg, J.C., Casas-Sainz, A., de Vicente, G., Duarte, L.V., Fernàndez, M., Gómez, J.J., Gómez-Pugnaire, M.T., Sánchez, A.J., López-Gómez, J. & Macchiavelli, C., (2019).An introduction to the Alpine cycle in Iberia. In The Geology of Iberia: A Geodynamic Approach (pp. 1-14). Springer, Cham.

Vergés, J., & Fernàndez, M., (2012). Tethys–Atlantic interaction along the Iberia–Africa plate boundary: The Betic–Rif orogenic system. Tectonophysics, 579, 144–172.

Vergés, J., &Fernàndez, M., (2006). Ranges and basins in the Iberian Peninsula: Their contribution to the present topography. Geol. Soc. Mem., 32, 223–234.

Vergés, J., &Sàbat, F., (1999). Constraints on the western Mediterranean kinematic evolution along a 1,000-km transect from Iberia to Africa. In: Durand, B., Jolivet, L., Horváth, F., Séranne, M. (Eds.), On the Mediterranean Basins: Tertiary Extension within Alpine orogen. Geological Society London Special Publications, 134, pp. 63–80.

Vidal, N., Gallart, J., &Dañobeitia, J.J., (1998). A deep seismic transect from the NE Iberian Peninsula to the Western Mediterranean. Journal of Geophysical Research 103, 12381–12396.

Vilà, M., Fernàndez, M., & Jiménez-Munt, I. (2010). Radiogenic heat production variability of some common lithological groups and its significance to lithospheric thermal modeling.Tectonophysics, 490,152–164. https://doi.org/10.1016/j.tecto.2010.05.003

Villaseñor, A., Chevrot, S., Harnafi, M., Gallart, J., Pazos, A., Serrano, I., et al. (2015). Subduction and volcanism in the Iberia-North Africa collision zone from tomographic images of the upper mantle.Tectonophysics, 663, 238–249. https://doi.org/10.1016/j.tecto.2015.08.042

Villaseca, C., Ancochea, E., Orejana, D., & Jeffries, T. (2010). Composition and evolution of the lithospheric mantle in central Spain: Inferences from peridotite xenoliths from the Calatrava volcanic field. Geological Society ofLondon, Special Publication, 337, 125–152. https://doi.org/10.1144/sp3377

Wilson, M., &Bianchini, G., (1999).Tertiary–Quaternary magmatismwithin the Mediterranean and surrounding regions. In: Durand,B., Jolivet, L., Horvath, F., Séranne, M. (Eds.), The Mediterranean Basins: Tertiary Extension within the Alpine Orogen.Geol. Soc., London Spec. Publ., vol. 156, pp. 141–168.

Workman, R., & Hart, S. (2005). Major and trace element composition of the depleted MORB mantle (DMM). Earth and Planetary Science Letters, 231 (1-2), 53-72.

Zeyen, H., P. Ayarza, M. Fernàndez, & A. Rimi (2005), Lithospheric structure under the western African-European plate boundary: A transect across the Atlas Mountains and the Gulf of Cadiz. Tectonics, 24, TC2001, doi:10.1029/2004TC001639.

13. Supplementary information references

Augier, R., Agard, P., Monié, P., Jolivet, L., Robin, C., &Booth-Rea, G., (2005). Exhumation, doming and slab retreat in the Betic Cordillera (SE Spain): in situ 40Ar/39Ar ages and P–T–d–t paths for the Nevado-Filabride complex. Journal of Metamorphic Geology 23, 357–381.

Azañón, J.M., &Crespo-Blanc, A., (2000). Exhumation during a continental collision inferred from the tectonometamorphic evolution of the Alpujarride Complex in the central Betics (Alboran Domain, SE Spain). Tectonics 19, 549–565.

Katz, R. F., M. Spiegelman, & C. H. Langmuir, (2003). A new parameterization of hydrous mantle melting, Geochem.Geophys.Geosyst., 4(9), 1073, doi:10.1029/2002GC000433.

López Sánchez-Vizcaíno, V., Rubatto, D., Gómez-Pugnaire, M.T., Trommsdorff, V., &Müntener, O., (2001).Middle Miocene high-pressure metamorphism and fast exhu- mation of the Nevado-Filábride Complex, SE Spain. Terra Nova 13, 327–332.

Massonne, H. J., Willner, A. P., &Gerya, T. (2007). Densities of metapelitic rocks at high to ultrahigh pressure conditions: What are the geodynamic consequences?. *Earth and Planetary Science Letters*, *256*(1-2), 12-27.

Puga, E., Nieto, J.M., &Díaz De Federico, A., (2000). Contrasting P–T Paths in eclogites of the Betic Ophiolitic Association, Mulhacen Complex, Southeastern Spain. The Canadian Mineralogist 38, 1137–1161.

Rudnick, R. L., & Gao, S. (2003). Composition of the continental crust.Treatise on Geochemistry, 3, 659. https://doi.org/10.1016/B0-08-043751-6/03016-4

Journal of Geophysical Research-Solid Earth

Supporting Information for

Opposite symmetry in the lithospheric structure of the Alboran and Algerian basins and their margins (Western Mediterranean): Geodynamic implications

Ajay Kumar[1, 2], Manel Fernàndez[1], Jaume Vergés[1], Montserrat Torne[1], Ivone Jiménez-Munt[1]

[1]Group of Dynamics of the Lithosphere, Geosciences Barcelona,GEO3BCN-CSIC, Lluís Solé Sabarís s/n, 08028 Barcelona, Spain.

[2]Department of Earth and Ocean Dynamics, University of Barcelona, Barcelona, Spain.

Contents of this file

Figures S1 to S8

Introduction

This file includes eight supplementary figures which are used to support the main text in the manuscript.

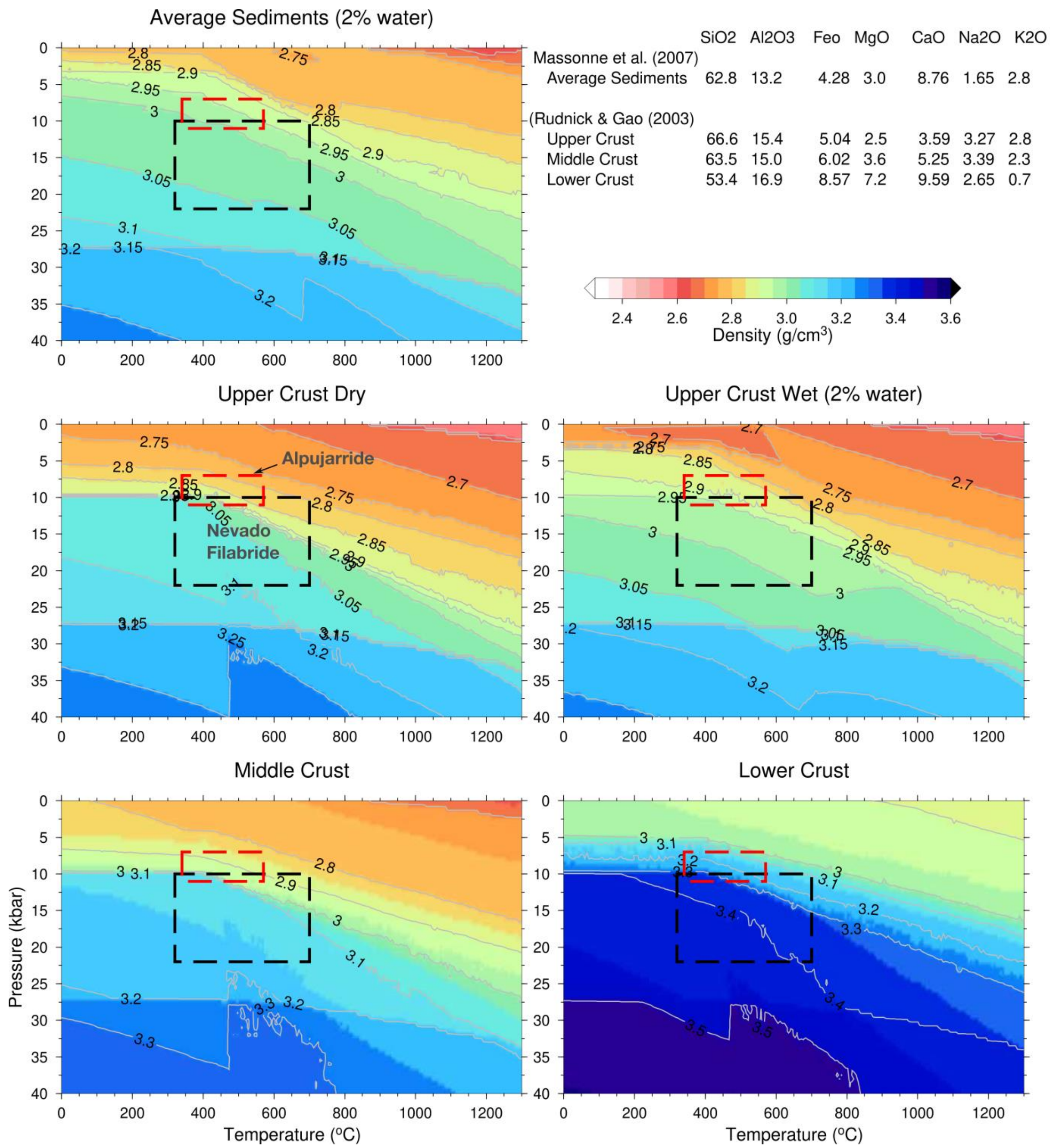

Figure S1. Pressure and Temperature dependent density distribution from average major oxides composition of sediments, upper crust, middle crust and lower crust (see the legend), resulting from stable phases and mineral assemblages computed using the Gibbs free-energy minimization algorithm (Connolly, 2005,2009). Red and black dashed line boxes mark the range of high pressure metamorphic peaks for Alpujarride and Nevado-Filabride, respectively, determined from thermo-barometry (Augier et al., 2005; López Sánchez- Vizcaíno et al., 2001; Puga et al., 2000; Azañón and Crespo-Blanc, 2000).

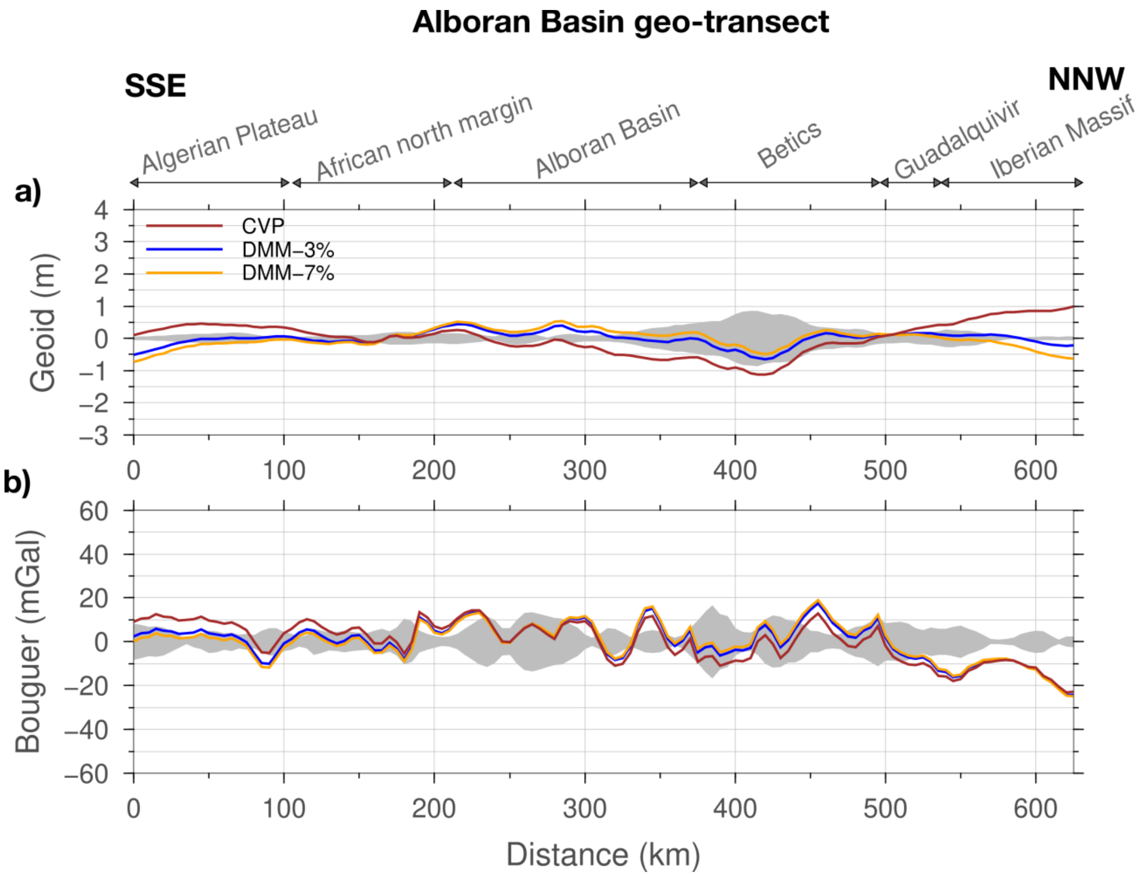

Figure S2. Sensitivity test for variations in the chemical composition of the Alboran slab to (a) geoid height and (b) Bouguer anomaly. Variation in chemical composition has minuscule effect on the Bouguer anomaly and has noticeable effect on the geoid height. Variation in the Alboran slab composition, situated at depths >140 km, changes the mass distribution in the slab region and consequently affects the geoid at longer wavelengths along the geo-transect. DMM-3% chemical composition fits the geoid better along the Alboran Basin geo-transect.

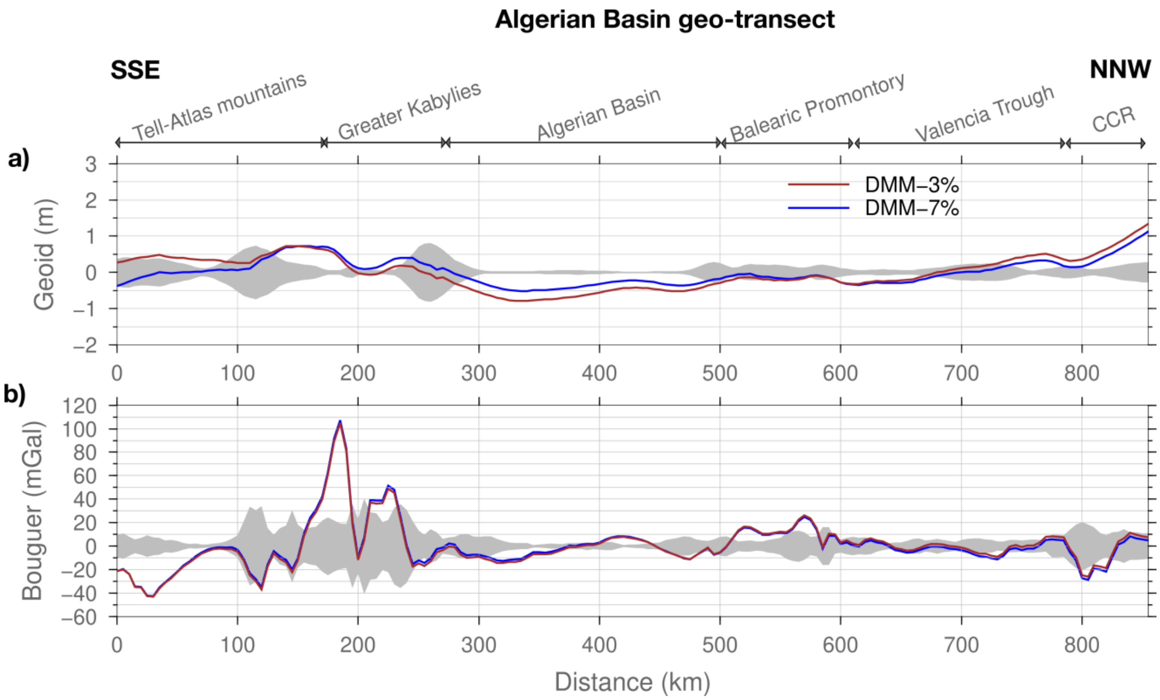

Figure S3. Sensitivity test for variations in the chemical composition of the Algerian slab to (a) geoid height and (b) Bouguer anomaly. DMM-7% chemical composition, resulting from 7% decompressional melting of DMM, fits the geoid better along the Algerian Basin geo-transect. CCR, Catalan Coastal Ranges.

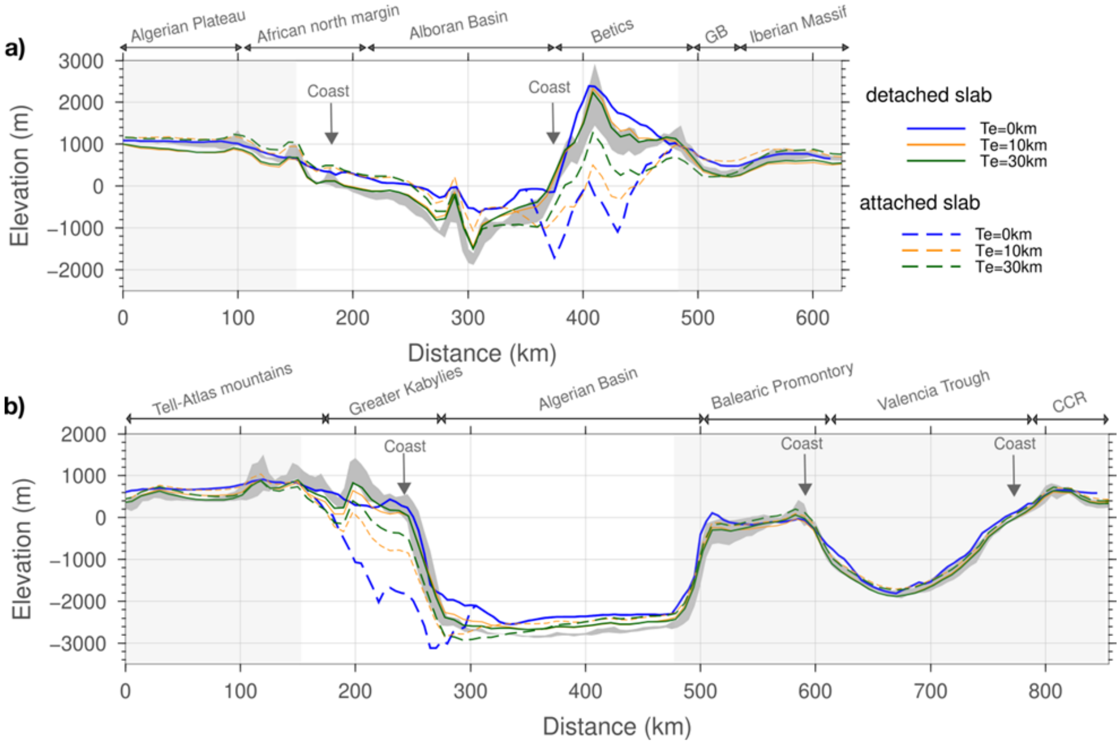

Figure S4. Observed and modeled elevation across the (a) Alboran Basin and (b) Algerian Basin geo-transect. Region highlighted in white shows extend along the geo-transect to which the slabs would affect the elevation. Dark-grey shaded strip shows the observed elevation across 50 km wide swath along the geo-transects. Solid colored lines represent calculated elevation with no slab anomaly, while dashed color lines show calculated elevation considering the slab. Blue line shows isostatic elevation (i.e. Te = 0 km). Orange and green lines show elevation considering flexural isostasy, Te = 10 km, and 30 km, respectively.

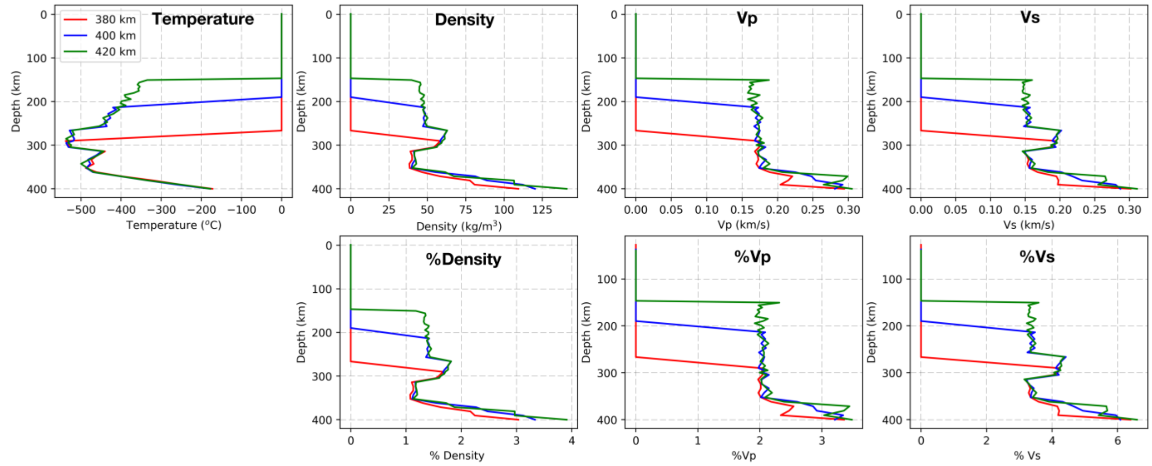

Figure S5. Temperature, density, and P- and S-wave velocity depth distribution in the Alboran slab at three locations spanning the slab region along the Alboran Basin geo-transect (see the legend). Upper panel shows the absolute deviation with respect to the LitMod reference column (Kumar et al., 2020) and lower panel shows the percentage change.

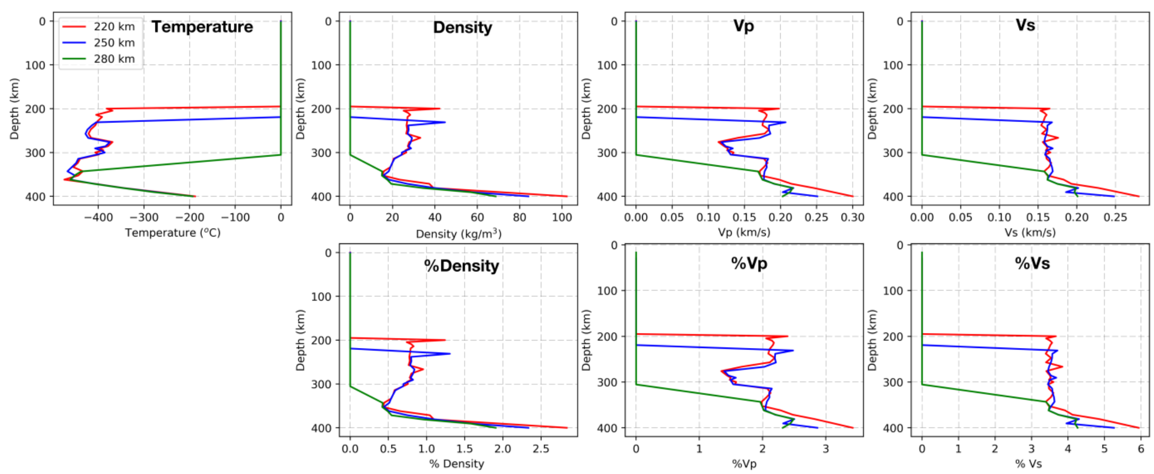

Figure S6. Temperature, density, and P- and S-wave velocity depth distribution in the Algerian slab at three locations spanning the slab region along the Algerian Basin geo-transect (see the legend). Upper panel shows the absolute deviation with respect to the LitMod reference column (Kumar et al., 2020) and lower panel shows the percentage change.

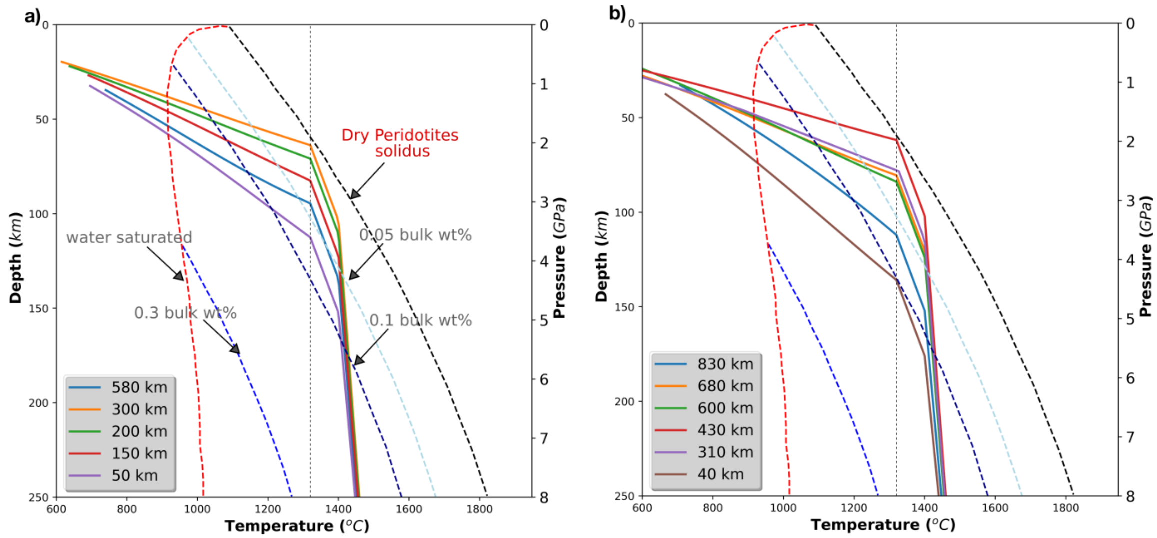

Figure S7. Geotherms at selected locations along (a) the Alboran basin and (b) the Algerian basin geo-transects. Dry and wet peridotite solidus for different amount of bulk water from Katz et al. (2003) are also plotted to indicate the presence of partial melts.

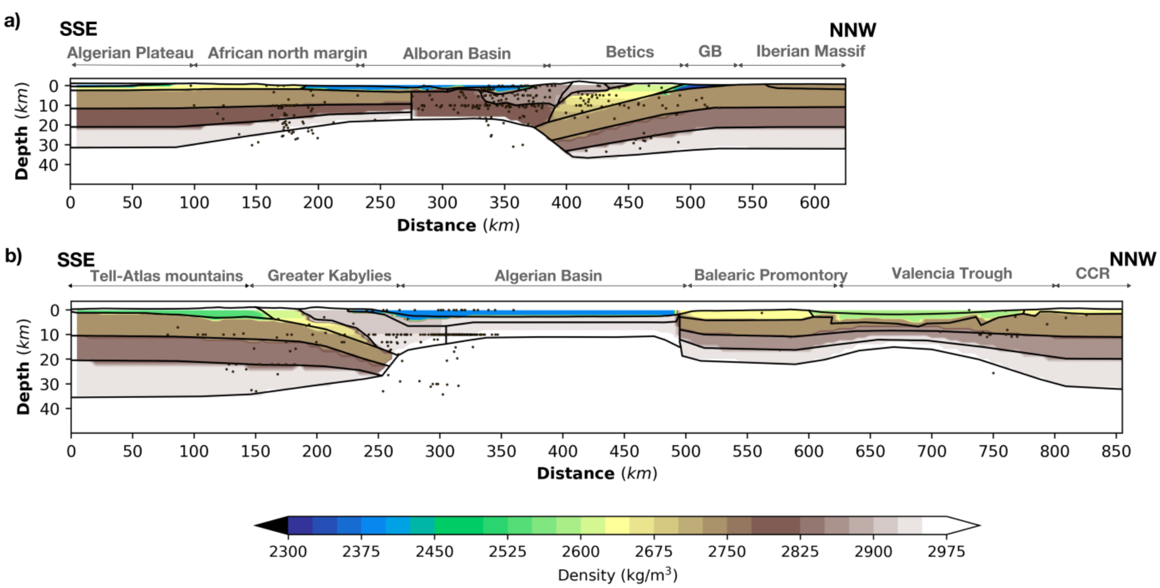

Figure S8. Crustal density distribution along the (a) Alboran Basin and (b) Algerian Basin geo-transects. Seismicity is also plotted (See Figure 4 in the main text for legend). Note the increasing density with depth in the External Units reaching values close to the upper crust.